

# Gravitational Wave Propagation in K-essence Cosmology: Theory and Observational Constraints

Sougata Bhunia,<sup>1,\*</sup> Eduardo Guendelman,<sup>2,3,4,†</sup> Debashis Gangopadhyay,<sup>5,‡</sup>  
Ramón Herrera,<sup>6,§</sup> Abhijit Bhattacharyya,<sup>1,¶</sup> and Goutam Manna<sup>a7,8,\*\*</sup>

<sup>1</sup>*Department of Physics, University of Calcutta, 92, A.P.C. Road, Kolkata-700009, India*

<sup>2</sup>*Department of Physics, Ben-Gurion University of the Negev, Beer-Sheva, Israel*

<sup>3</sup>*Frankfurt Institute for Advanced Studies (FIAS),*

*Ruth-Moufang-Strasse 1, 60438 Frankfurt am Main, Germany.*

<sup>4</sup>*Bahamas Advanced Study Institute and Conferences, 4A Ocean Heights,  
Hill View Circle, Stella Maris, Long Island, The Bahamas.*

<sup>5</sup>*Department of Physics, School of Natural Sciences, Sister Nivedita University,  
DG 1/2, Action Area 1, Newtown, Kolkata 700156, India.*

<sup>6</sup>*Instituto de Física, Pontificia Universidad Católica de Valparaíso,  
Avenida Brasil 2950, Casilla 4059, Valparaíso, Chile.*

<sup>7</sup>*Department of Physics, Prabhat Kumar College, Contai, Purba Medinipur 721404, India*

<sup>8</sup>*Institute of Astronomy, Space and Earth Science, Kolkata 700054, India*

(Dated: May 26, 2026)

Gravitational waves (GWs) provide a powerful, theory-independent probe of the dynamical structure of spacetime and the cosmological background. We study linearized GW propagation in k-essence cosmology, where a non-canonical scalar field describes the dark sector. In the high-frequency (short-wavelength) approximation on a Friedmann–Lemaître–Robertson–Walker (FLRW) background, and restricting to the transverse-traceless tensor sector, we derive a modified evolution equation for tensor perturbations. The GW speed remains strictly luminal, consistent with multimessenger bounds such as GW170817, but the interaction with the background field  $\bar{\phi}$  induces a time-dependent effective mass-like term  $m_{\text{eff}}$ . This background-induced mass modifies the dispersion relation without introducing additional propagating degrees of freedom, leading to a cumulative, frequency-dependent phase shift in the waveform over cosmological distances. We show that  $m_{\text{eff}}$  is uniquely determined by background cosmological parameters and can be written as a redshift-dependent function,  $m_{\text{eff}}(z)$ , directly linking GW observables to scalar-field dynamics, while the GW luminosity distance remains identical to its electromagnetic counterpart, preserving standard-siren consistency. We test the scenario through a joint Bayesian analysis that combines cosmic chronometers (CC), BAO, Pantheon+SH0ES, and standard-siren data from GWTC-2.1/3/4. The reconstruction is consistent with current constraints and reproduces the late-time expansion history, while the evolution of  $m_{\text{eff}}(z)$  offers a new mechanism that may help alleviate the  $H_0$  tension.

Keywords: Gravitational waves, Linearized gravity, k-essence cosmology, observational constraints

## I. INTRODUCTION

The theoretical prediction of gravitational waves (GWs) dates back to the formulation of General Relativity (GR), where Einstein showed that the linearized field equations admit propagating perturbations of the spacetime metric [1]. Later work placed gravitational radiation on firm physical ground by clarifying its generation and energy transport in curved spacetime [2, 3]. Indirect evidence was provided by the observed orbital decay of the binary pulsar PSR B1913+16, in remarkable agreement with the GR prediction [4, 5]. A century after their prediction, the first direct detection—the binary black-hole merger GW150914—opened the era of gravitational-wave astronomy [6]. Since then, successive GW catalogs [7–11] have established gravitational physics as an observational science and provided

unique access to the dynamical sector of spacetime. Beyond their astrophysical impact, GWs also offer powerful cosmological probes. In particular, standard sirens [12, 13] enable direct distance measurements that are independent of the electromagnetic distance ladder, providing a complementary route to constrain the expansion history of the universe and the properties of its dominant components.

Within GR, gravitational waves can be described as massless tensor perturbations propagating on a background spacetime: they satisfy a dispersionless wave equation and travel at the speed of light [14, 15]. In a cosmological setting based on the Friedmann–Lemaître–Robertson–Walker (FLRW) metric, the expansion of the universe primarily affects GWs through an adiabatic damping of their amplitude as they travel over cosmological distances. This picture has been tested stringently by the multi-messenger observation of the binary neutron-star merger GW170817 [16] and its electromagnetic counterpart GRB 170817A [17], which constrains any deviation between the propagation speed of GWs and light to be extremely small. However, while such measurements severely limit modifications to the speed of gravity, they do not exclude subtler propagation effects induced by the cosmological background, in particular scenarios in which the dispersion

\* sougatabhunia066@gmail.com

† guendel@bgu.ac.il

‡ debashis.g@snuniv.ac.in

§ ramon.herrera@pucv.cl

¶ abhattacharyyacu@gmail.com

\*\* goutammanna.pkc@gmail.com

<sup>a</sup>Corresponding author

properties of the waves are modified without changing their (low-frequency) propagation speed [18, 19].

A broader and more systematic framework for scalar–tensor theories is provided by Horndeski gravity, the most general scalar–tensor theory with second-order field equations and free from Ostrogradsky instabilities [20, 21, 68]. In this class of theories, derivative couplings between the scalar field and curvature can modify both the background cosmological evolution and the propagation of gravitational waves. Extensive work has explored these effects, showing that departures from GR may appear in the GW propagation speed, the effective amplitude damping, and the dispersion relation [18, 19, 23]. The tight bound on the GW speed from GW170817 [16], however, excludes large regions of the Horndeski parameter space, leaving viable only subclasses that predict (effectively) luminal propagation [24–26]. Within the surviving sector, k-essence (a subclass of the Horndeski gravity) provides a well-motivated limit in which the Lagrangian depends only on the scalar field and its kinetic term, with no explicit non-minimal coupling to curvature [27–29]. In this limit, modifications to GW propagation arise through the time-dependent cosmological background sourced by the scalar field.

The presence of such a non-trivial background raises a natural question: how does the dark sector influence the propagation of gravitational waves? Since GWs travel across cosmological distances, even small departures from standard propagation can accumulate into observable effects. In particular, modifications to the effective dispersion relation can induce frequency-dependent phase shifts in the waveform, providing a sensitive probe of the underlying cosmological medium [30, 31].

In this work, we study the linearized propagation of gravitational waves on a cosmological background sourced by a k-essence scalar field. A central theoretical challenge is the consistent definition of perturbations on a curved, time-dependent spacetime, where the split between background and fluctuations is not unique. We address this issue by working in the *short-wavelength (high-frequency) approximation*, in which GWs are rapidly varying perturbations with wavelength much smaller than the characteristic curvature scale of the background [32, 33]. Within this framework, we derive the linearized Einstein equations in the presence of k-essence, treating the metric and scalar field as independent dynamical degrees of freedom. By adopting unitary gauge (suppressing intrinsic scalar perturbations), we isolate the impact of the k-essence background on the tensor sector. We show that, although the GW propagation speed remains strictly luminal, the combined effects of cosmological expansion and the non-canonical scalar dynamics generate an effective mass-like term in the GW equation.

We consider models described by a non-canonical Lagrangian  $\mathcal{L}(X, \phi)$ . For transverse–traceless tensor modes on an FLRW background, we derive the modified evolution equation and show that the effective mass alters the dispersion relation without introduc-

ing additional propagating degrees of freedom. This modification accumulates into a frequency-dependent phase shift in GW signals over cosmological distances, providing an observational signature absent in standard GR and qualitatively distinct from scenarios that modify the propagation speed or the amplitude damping [18, 25]. Importantly, the effective mass can be expressed in terms of cosmological quantities such as the Hubble rate and the scalar-field equation of state, thereby linking GW observables directly to the physics of dark energy.

This work highlights the role of gravitational waves as precision probes of the cosmological background, showing that tensor perturbations can encode subtle signatures of the dark sector. As GW observations continue to improve in sensitivity and redshift reach, these effects offer a promising avenue to test the microphysics of dark energy and to explore possible departures from the standard cosmological paradigm.

The paper is organized as follows. In Section II, we present the theoretical framework for gravitational-wave propagation in curved spacetime. In Section III, we introduce the k-essence scalar-field model, derive the background cosmological equations, and review linear perturbations on an FLRW background. In Section IV, we obtain the modified gravitational-wave evolution equation in the presence of the k-essence field, highlighting the emergence of an effective mass term and its implications for the dispersion relation. In Section V, we describe our methodology for confronting the model with observational data. In Section VI, we fit the model to several datasets—*Cosmic Chronometers (CC)*, *Pantheon+SHOES*, *Baryon Acoustic Oscillations (BAO)*, and *Gravitational-Wave Transient Catalogs (GWTC; GWTC-2.1, GWTC-3, and GWTC-4)*—and discuss the results. Section VII concludes with a summary of our findings.

## II. REVIEW OF LINEARIZED GRAVITY THEORY FOR CURVED BACKGROUND SPACETIME

Our analysis begins by formulating the equation for metric perturbation in a general curved and dynamical background spacetime, the solutions of which ultimately yield the gravitational wave profile for the given geometry. That means in our consideration, the background stress-energy tensor is non-zero. So, the perturbed metric can be written as [14, 34–38]

$$g_{\mu\nu}(x) = \bar{g}_{\mu\nu}(x) + h_{\mu\nu}(x), \quad \|h_{\mu\nu}\| \ll 1. \quad (1)$$

where  $h_{\mu\nu}(x)$  is a small metric perturbation to the background curved spacetime metric  $\bar{g}_{\mu\nu}$ , which also can be defined as  $h_{\mu\nu} \equiv \delta g_{\mu\nu}$ .

A natural question in the decomposition of Eq. (1) is how to distinguish the curved background  $\bar{g}_{\mu\nu}$  from the perturbation  $h_{\mu\nu}$  in a generic spacetime. Unlike the flat-spacetime case, this split is neither unique nor intrinsically meaningful; rather, it is defined operationally through a separation of scales [14]. We identify  $\bar{g}_{\mu\nu}$  with the slowly varying part of the metric on

length scales much larger than the gravitational-wave wavelength, while  $h_{\mu\nu}$  captures the rapidly varying, small-amplitude fluctuations. Consequently, the distinction is gauge-dependent and becomes well-defined only after an appropriate averaging over spacetime regions (or wavelengths).

This decomposition is essential for a consistent description of gravitational waves beyond flat spacetime. In particular, it permits the construction of an effective energy–momentum tensor from second-order perturbations, which acts as a source for the background geometry. Gravitational waves therefore propagate on  $\bar{g}_{\mu\nu}$  while also inducing a backreaction on it, making this framework central to studies of GW propagation, energy transport, and their role in curved and cosmological spacetimes.

In the present work, we restrict attention to terms linear in  $h_{\mu\nu}$ . While the split  $g_{\mu\nu} = \bar{g}_{\mu\nu} + h_{\mu\nu}$  is unambiguous on a Minkowski background, it is more delicate on a generic curved spacetime because both  $\bar{g}_{\mu\nu}$  and  $h_{\mu\nu}$  vary with position. We therefore work in the short-wavelength (high-frequency) regime, where the perturbation wavelength  $\lambda$  is much smaller than the characteristic curvature scale  $L$  of the background [14, 39]. The combined weak-field and short-wavelength assumptions ( $|h_{\mu\nu}| \ll 1$ ,  $\lambda \ll L$ ) provide a consistent framework for gravitational-wave propagation in cosmological spacetimes: the perturbations behave as linear, rapidly varying modes on a slowly varying background geometry. In this limit, the leading contribution to the first-order correction of the Christoffel symbols,  $\Gamma^{(1)}$ , is dominated by the short-wavelength modes.

Accordingly, we neglect all higher-order terms  $\mathcal{O}(h^2)$ , thereby discarding the nonlinear contributions that would otherwise generate an effective energy–momentum tensor for gravitational waves and their backreaction on the background spacetime. We also set the first-order matter perturbations to zero,  $T_{\mu\nu}^{m(1)} = 0$ , so that the dynamics are governed solely by linearized geometric perturbations propagating on a fixed curved background. This *weak-field, high-frequency approximation* is standard in analyses of gravitational-wave propagation in cosmological spacetimes.

The inverse metric  $g^{\mu\nu}$  can be expressed as [14, 39]

$$g^{\mu\nu}(x) = \bar{g}^{\mu\nu}(x) - h^{\mu\nu}(x) + \mathcal{O}(h^2). \quad (2)$$

The Christoffel symbol ( $\Gamma_{\nu\rho}^{\mu}$ ) with a linearized order perturbation is expressed as

$$\Gamma_{\nu\rho}^{\mu} = \bar{\Gamma}_{\nu\rho}^{\mu} + \delta\Gamma_{\nu\rho}^{\mu}, \quad (3)$$

where  $\bar{\Gamma}_{\nu\rho}^{\mu}$  is associated with the background metric  $\bar{g}_{\mu\nu}$  and the linearly perturbed connection coefficient has the following form [14],

$$\delta\Gamma_{\nu\rho}^{\mu} = \Gamma_{\nu\rho}^{\mu(1)} = \frac{1}{2}\bar{g}^{\mu\sigma}(\bar{\nabla}_{\nu}h_{\rho\sigma} + \bar{\nabla}_{\rho}h_{\nu\sigma} - \bar{\nabla}_{\sigma}h_{\nu\rho}). \quad (4)$$

It is to note that here,  $\bar{\nabla}_{\mu}$  is the covariant derivative with respect to background metric  $\bar{g}_{\mu\nu}$  and mention the condition of metric compatibility  $\bar{\nabla}_{\lambda}\bar{g}_{\mu\nu} = 0$ .

The Ricci tensor can be split into background, and linearly perturbed Ricci tensor as

$$R_{\mu\nu} = (\bar{R}_{\mu\nu} + R_{\mu\nu}^{(1)}), \quad (5)$$

where the linearized Ricci tensor is [14]

$$R_{\mu\nu}^{(1)} = \frac{1}{2}(\bar{\nabla}_{\alpha}\bar{\nabla}_{\mu}h_{\nu}^{\alpha} + \bar{\nabla}_{\alpha}\bar{\nabla}_{\nu}h_{\mu}^{\alpha} - \bar{\square}h_{\mu\nu} - \bar{\nabla}_{\mu}\bar{\nabla}_{\nu}h), \quad (6)$$

where  $h = h_{\lambda}^{\lambda}$  is the stress of the metric perturbation and  $\bar{\square} = \bar{g}^{\mu\nu}\bar{\nabla}_{\mu}\bar{\nabla}_{\nu}$ . The notable thing is that  $\bar{\nabla}_{\nu}\bar{\nabla}_{\mu}h = \bar{\nabla}_{\nu}\partial_{\mu}h = (\partial_{\nu}\partial_{\mu}h - \bar{\Gamma}_{\nu\rho}^{\rho}\partial_{\rho}h)$  is symmetric under the exchange  $\mu \leftrightarrow \nu$  and therefore  $R_{\mu\nu}^{(1)}$  is also symmetric [14].

For algebraic simplification, we have used the trace-reversed perturbation variable which can be defined as [14, 39]

$$\tilde{h}_{\mu\nu} = h_{\mu\nu} - \frac{1}{2}\bar{g}_{\mu\nu}h, \quad (7)$$

with the trace of metric perturbation

$$\tilde{h} = -h. \quad (8)$$

Therefore, we can write

$$\begin{aligned} h_{\mu\nu} &= \tilde{h}_{\mu\nu} - \frac{1}{2}\bar{g}_{\mu\nu}\tilde{h} \\ h_{\nu}^{\alpha} &= \tilde{h}_{\nu}^{\alpha} - \frac{1}{2}\delta_{\nu}^{\alpha}\tilde{h} \end{aligned} \quad (9)$$

In the present analysis, we work in the weak-field, high-frequency regime of linearized gravity. It is therefore convenient to introduce the trace-reversed perturbation, which removes redundant trace terms and simplifies the linearized Einstein equations. In this form the field equations become effectively diagonal, making the propagating degrees of freedom manifest and allowing the dynamics to be cast as a relativistic wave equation for metric perturbations (i.e., gravitational waves).

Since  $R_{\mu\nu}^{(1)}$  is symmetric under  $\mu \leftrightarrow \nu$ , the corresponding second derivatives commute, so that  $\bar{\nabla}_{\nu}\bar{\nabla}_{\mu}\tilde{h} = \bar{\nabla}_{\mu}\bar{\nabla}_{\nu}\tilde{h}$ .

For gravitational waves on a curved background, it is convenient to impose the Lorentz (Hilbert/harmonic/De Donder) gauge [14, 34–38], which partially fixes the coordinate freedom and removes unphysical components of the metric perturbation. With this choice, the linearized field equations take a simpler wave-like form. On a curved background, the gauge condition is [39]:

$$\bar{\nabla}_{\mu}\tilde{h}^{\mu\nu} = 0 \quad (10)$$

Therefore, the linearly perturbed Ricci tensor becomes

$$R_{\mu\nu}^{(1)} = \frac{1}{2}\left[\bar{\nabla}_{\alpha}\bar{\nabla}_{\mu}\tilde{h}_{\nu}^{\alpha} + \bar{\nabla}_{\alpha}\bar{\nabla}_{\nu}\tilde{h}_{\mu}^{\alpha} - \bar{\square}\tilde{h}_{\mu\nu} + \frac{1}{2}\bar{g}_{\mu\nu}(\bar{\square}\tilde{h})\right]. \quad (11)$$

and the linearized Ricci scalar can be written as

$$R^{(1)} = \frac{1}{2}\bar{\square}\tilde{h} + \bar{R}^{\mu\nu}\tilde{h}_{\mu\nu} + \frac{1}{2}\bar{R}\tilde{h} \quad (12)$$

According to the definition of the Einstein tensor  $E_{\mu\nu}$  ( $= R_{\mu\nu} - \frac{1}{2}g_{\mu\nu}R$ ), where  $E_{\mu\nu}$  denotes the Einstein tensor for notational convention. Now we can split the Einstein tensor into the two parts, as the background and the linearly perturbed parts, as follows

$$E_{\mu\nu} = \bar{E}_{\mu\nu} + E_{\mu\nu}^{(1)}. \quad (13)$$

The linearly perturbed form of the Einstein tensor can be written as

$$E_{\mu\nu}^{(1)} = R_{\mu\nu}^{(1)} - \frac{1}{2}\bar{g}_{\mu\nu}R^{(1)} - \frac{1}{2}h_{\mu\nu}\bar{R}. \quad (14)$$

Thus, putting the values of  $R_{\mu\nu}^{(1)}$  and  $R^{(1)}$  from Eqs. (11) and (12) and trace-reversed term of the metric perturbation from Eqs. (8) and (9), we get

$$E_{\mu\nu}^{(1)} = \left[ -\frac{1}{2}\bar{\square}h_{\mu\nu} + \bar{R}_{\alpha\mu\nu\beta}\tilde{h}^{\alpha\beta} + \frac{1}{2}(\bar{R}_{\lambda\mu}\tilde{h}_{\nu}^{\lambda} + \bar{R}_{\lambda\nu}\tilde{h}_{\mu}^{\lambda}) - \frac{1}{2}\bar{g}_{\mu\nu}(\bar{R}^{\alpha\beta}\tilde{h}_{\alpha\beta}) - \frac{1}{2}\tilde{h}_{\mu\nu}\bar{R} \right] \quad (15)$$

This is the final expression for the Einstein tensor to linear order in the perturbation, combining contributions from the linearized Einstein equations and the gravitational-wave equation.

### III. SCALAR-INDUCED GRAVITATIONAL WAVES

In this section, we derive the linearized gravitational-wave equation in the presence of a k-essence scalar field, including both scalar and tensor perturbations.

#### A. Linearized Perturbation in Scalar Field Model

The action we have considered, where a scalar field is involved with a curved background metric [28, 29, 40–47, 49–53]

$$S = \int d^4x \sqrt{-g} \left[ \frac{R}{2\kappa^2} + \mathcal{L}(X, \phi) \right] \quad (16)$$

where  $\kappa^2 = 8\pi G$ ,  $\mathcal{L}(X, \phi)$  is the non-canonical Lagrangian,  $g$  is the determinant of the metric involved,  $X \equiv \frac{1}{2}g^{\mu\nu}\partial_{\mu}\phi\partial_{\nu}\phi$  represents canonical kinetic term and  $\phi$  is the k-essence scalar field.

We begin with the scalar field  $\phi$ , which in general depends on both time and space,  $\phi \equiv \phi(t, \mathbf{x})$ . Introducing small perturbations about a homogeneous background, we decompose  $\phi$  into a spatially independent background and a perturbation [29, 34, 54]:

$$\phi(t, x) = \bar{\phi}(t) + \delta\phi(t, x) \quad (17)$$

where the background field  $\bar{\phi}$  is only the function of time since our background universe is homogeneous in nature, and  $|\delta\phi| \ll \bar{\phi}$ .

Here, the spacetime metric  $g_{\mu\nu}$  and the k-essence scalar field  $\phi$  are independent dynamical fields in the

action. Accordingly, their perturbations  $h_{\mu\nu}$  and  $\delta\phi$  are defined independently and can be expanded about their respective background configurations, without assuming any direct algebraic relation between them.

Since we work at linear order, we retain only terms that are first order in  $h_{\mu\nu}$  or  $\delta\phi$  and neglect all quadratic and mixed contributions (e.g.,  $h\delta\phi$ ).

Therefore, the variation of the kinetic term can be derived as,

$$\delta X = \left[ -\frac{1}{2}h^{\mu\nu}\partial_{\mu}\bar{\phi}\cdot\partial_{\nu}\bar{\phi} \right] + \bar{g}^{\mu\nu} \left[ \partial_{\mu}(\delta\phi)\cdot\partial_{\nu}\bar{\phi} \right] \quad (18)$$

or,  $\delta X = \delta X_h + \delta X_{\phi}$

where, we have defined  $\delta X_h = (-\frac{1}{2}h^{\mu\nu}\partial_{\mu}\bar{\phi}\cdot\partial_{\nu}\bar{\phi})$  and  $\delta X_{\phi} = \bar{g}^{\mu\nu}[\partial_{\mu}(\delta\phi)\cdot\partial_{\nu}\bar{\phi}]$ .

The energy-momentum tensor of the k-essence scalar field (see Appendix A) is

$$T_{\mu\nu}^{\phi} = g_{\mu\nu}\mathcal{L} - \mathcal{L}_X\partial_{\mu}\phi\partial_{\nu}\phi, \quad (19)$$

where  $\mathcal{L}_X \equiv \partial\mathcal{L}/\partial X$ ,  $\mathcal{L}_{X\phi} \equiv \partial^2\mathcal{L}/(\partial X\partial\phi)$ ,  $\mathcal{L}_{XX} \equiv \partial^2\mathcal{L}/\partial X^2$ , and  $\mathcal{L}_{\phi} \equiv \partial\mathcal{L}/\partial\phi$ .

Thus, the linearly perturbed energy-momentum tensor can be expressed as

$$\delta T_{\mu\nu}^{\phi} \equiv T_{\mu\nu}^{\phi(1)} = M_{\mu\nu}(h) + S_{\mu\nu}(\delta\phi) \quad (20)$$

where,  $M_{\mu\nu}(h)$  depends on metric perturbation term  $h_{\mu\nu}$  in linear order and can be defined as

$$M_{\mu\nu}(h) \equiv [h_{\mu\nu}\mathcal{L} + \bar{g}_{\mu\nu}\mathcal{L}_X(\delta X_h)\mathcal{L} - \mathcal{L}_{XX}(\delta X_h)\partial_{\mu}\bar{\phi}\cdot\partial_{\nu}\bar{\phi}] \quad (21)$$

and the second term in Eq.(20), i.e.,  $S_{\mu\nu}(\delta\phi)$  depends on the scalar field perturbation term  $\delta\phi$  and defined as

$$S_{\mu\nu}(\delta\phi) \equiv [\bar{g}_{\mu\nu}\mathcal{L}_X(\delta X_{\phi}) + \bar{g}_{\mu\nu}\mathcal{L}_{\phi}(\delta\phi) - \mathcal{L}_{XX}(\delta X_{\phi})\partial_{\mu}\bar{\phi}\cdot\partial_{\nu}\bar{\phi} - \mathcal{L}_{X\phi}(\delta\phi)\partial_{\mu}\bar{\phi}\cdot\partial_{\nu}\bar{\phi} - \mathcal{L}_X(\partial_{\mu}(\delta\phi)\cdot\partial_{\nu}\bar{\phi} + \partial_{\nu}(\delta\phi)\cdot\partial_{\mu}\bar{\phi})] \quad (22)$$

Note that Eqs. (21) and (22) show that the two contributions to the linearized energy-momentum tensor in Eq. (20) depend separately on  $h_{\mu\nu}$  and  $\delta\phi$ ; there are no mixed terms proportional to  $h_{\mu\nu}\delta\phi$  at this order.

Combining Eqs. (14) and (20), the linearized Einstein equation takes the form

$$E_{\mu\nu}^{(1)} \equiv 8\pi G T_{\mu\nu}^{\phi(1)} \equiv 8\pi G [M_{\mu\nu}(h) + S_{\mu\nu}(\delta\phi)], \quad (23)$$

where we have set  $T_{\mu\nu}^{m(1)} = 0$ .

Using Eqs. (7)–(9),  $\delta X_h$  can be expressed in terms of the trace-reversed variable as

$$\delta X_h = -\delta X_{\bar{h}} + \frac{1}{2}\bar{X}\tilde{h}, \quad (24)$$

where  $\delta X_{\bar{h}} \equiv \frac{1}{2}\tilde{h}^{\mu\nu}\partial_{\mu}\bar{\phi}\partial_{\nu}\bar{\phi}$  and  $\bar{X} \equiv \frac{1}{2}\bar{g}^{\mu\nu}\partial_{\mu}\bar{\phi}\partial_{\nu}\bar{\phi}$ . Accordingly, Eq. (21) can be rewritten in terms of the trace-reversed perturbation as

$$M_{\mu\nu}(\tilde{h}) = \tilde{h}_{\mu\nu}\mathcal{L} - \bar{g}_{\mu\nu} \left[ \frac{1}{2}\tilde{h}\mathcal{L} + \mathcal{L}_X \left( \frac{1}{2}\bar{X}\tilde{h} - \delta X_{\bar{h}} \right) \right] + \partial_{\mu}\bar{\phi}\partial_{\nu}\bar{\phi} \left[ \mathcal{L}_{XX} \left( \delta X_{\bar{h}} - \frac{1}{2}\bar{X}\tilde{h} \right) \right] \quad (25)$$

In what follows we treat the k-essence field as a purely homogeneous background,  $\phi = \bar{\phi}(t)$ , and set its intrinsic perturbation to zero,  $\delta\phi = 0$ . At linear order (for a minimally coupled scalar), the transverse-traceless tensor sector evolves independently of scalar fluctuations [14, 34–38], so  $\delta\phi$  does not enter the tensor evolution equation directly; the scalar field influences the dynamics only through background quantities in the stress–energy tensor. This choice is analogous to working in unitary gauge, where the scalar perturbation is absorbed into the metric variables [55, 57, 58, 72].

With  $\delta\phi = 0$  we have  $\delta X_\phi = 0$ , and hence Eq. (22) implies  $S_{\mu\nu}(\delta\phi) = 0$ . Therefore, Eqs. (20) and (25) reduce to

$$T_{\mu\nu}^{\phi(1)} = M_{\mu\nu}(\tilde{h}) \quad (26)$$

Thus, at linear order, combining Eqs. (15), (23), and (26) yields *the linearized Einstein equation*:

$$\boxed{-\frac{1}{2}\bar{\square}\tilde{h}_{\mu\nu} + \tilde{W}_{\mu\nu} = 8\pi GM_{\mu\nu}(\tilde{h})} \quad (27)$$

where

$$\begin{aligned} \tilde{W}_{\mu\nu} = & \left[ \bar{R}_{\alpha\mu\nu\beta}\tilde{h}^{\alpha\beta} + \frac{1}{2}(\bar{R}_{\lambda\mu}\tilde{h}_\nu^\lambda + \bar{R}_{\lambda\nu}\tilde{h}_\mu^\lambda) \right. \\ & \left. - \frac{1}{2}\bar{g}_{\mu\nu}(\bar{R}^{\alpha\beta}\tilde{h}_{\alpha\beta}) - \frac{1}{2}\tilde{h}_{\mu\nu}\bar{R} \right] \quad (28) \end{aligned}$$

### B. Choice of Line Element with Scalar and Tensor Perturbation

In standard gravitational-wave theory on a flat or curved background, the metric perturbation  $h_{\mu\nu}$  contains both gauge (coordinate) degrees of freedom and physical, radiative degrees of freedom. The transverse-traceless (TT) gauge [14, 34–38] is particularly useful because it eliminates pure-gauge components and isolates the propagating tensor modes. Imposing appropriate gauge conditions and exploiting the residual coordinate freedom reduces the perturbation to its TT part, which is transverse to the direction of propagation and trace-free. Consequently, the gravitational wave is described by two independent polarization states, the plus (+) and cross (×) modes, which encode the measurable tidal distortions. In the present theory, Eq. (16) shows that the inclusion of a k-essence scalar field  $\phi$  in the Lagrangian  $\mathcal{L}(X, \phi)$  introduces additional physical but non-propagating (non-radiative) degrees of freedom in  $h_{\mu\nu}$ . As a result,  $h_{\mu\nu}$  cannot be made globally TT; instead, it can be decomposed into a radiative TT component that satisfies the TT conditions and complementary non-radiative pieces. The TT component obeys a wave equation in any frame, whereas the remaining components satisfy Poisson-type constraint equations, indicating that they are sourced and do not propagate as freely traveling radiation [15, 54].

We therefore consider scalar and tensor perturbations about an FLRW background ( $\bar{g}_{\mu\nu}$ ) and work in the conformal Newtonian (longitudinal) gauge with the (+, −, −, −) signature. In this gauge the scalar

shift and scalar shear are set to zero ( $B = E = 0$ ), so that the scalar sector is fully characterized by two potentials. We then adopt the perturbed line element [59–61]

$$ds^2 = a^2(\eta) \left[ (1 + 2\Phi)d\eta^2 - \left( (1 - 2\Psi)\delta_{ij} + \frac{1}{2}h_{ij}^{(TT)} \right) dx^i dx^j \right] \quad (29)$$

where  $\eta$  denotes conformal time and  $a(\eta)$  is the scale factor. In the Newtonian gauge,  $\Phi$  and  $\Psi$  coincide with the gauge-invariant Bardeen potentials [34]. The tensor  $h_{ij}^{(TT)}$  is the transverse-traceless perturbation describing gravitational waves, satisfying  $\partial^i h_{ij}^{(TT)} = 0$  and  $h^{(TT)i}_i = 0$ . The Newtonian gauge is applicable to linear perturbations about an FLRW background for modes with nonzero wavenumber and is particularly convenient when vector modes are neglected so that the metric can be cleanly decomposed into scalar and TT tensor sectors. In cosmological (including k-essence) backgrounds, the Bardeen potentials are gauge-invariant combinations of scalar metric perturbations that encode the physical scalar degrees of freedom; the analogous potentials in our framework play the same role, removing gauge artifacts and capturing the scalar dynamics sourced by the k-essence field. A non-vanishing scalar anisotropic stress leads to a gravitational slip,  $\Phi - \Psi \neq 0$ , which has been studied in detail (see, e.g., [74]).

Several works adopt the same perturbed metric in Eq. (29) and include scalar and tensor perturbations up to second order [59–61]. In contrast, since we focus on linear perturbation theory, we retain only first-order scalar and tensor perturbations and neglect vector modes as well as anisotropic stress [61].

Equation (29) implies the background conformal FLRW line element

$$d\bar{s}^2 = \bar{g}_{\mu\nu} dx^\mu dx^\nu = a^2(\eta) [d\eta^2 - \delta_{ij} dx^i dx^j] \quad (30)$$

and the corresponding nonvanishing perturbation components are obtained directly from Eq. (29):

$$\begin{aligned} h_{00} &= 2a^2(\eta)\Phi \\ h_{ij} &= -a^2(\eta) \left[ -2\Psi\delta_{ij} + \frac{1}{2}h_{ij}^{(TT)} \right] \\ h_{0i} &= 0 \end{aligned} \quad (31)$$

and the trace of that metric perturbation:

$$h = \bar{g}^{\mu\nu} h_{\mu\nu} = 2(\Phi - 3\Psi) \quad (32)$$

For algebraic convenience, we use Eqs. (7) and (8) to express the perturbations in Eqs. (31) and (32) in terms of the trace-reversed variable, yielding

$$\begin{aligned} \tilde{h}_{00} &= \left( h_{00} - \frac{1}{2}\bar{g}_{00}h \right) = a^2(\Phi + 3\Psi) \\ \tilde{h}_{ij} &= a^2(\Phi - \Psi)\delta_{ij} - \frac{a^2}{2}h_{ij}^{(TT)} \\ \tilde{h} &= -h = 2(3\Psi - \Phi) \end{aligned} \quad (33)$$

Since we work in conformal time  $\eta$ , we treat the homogeneous background scalar field as  $\bar{\phi} = \bar{\phi}(\eta)$ .

Using Eqs. (29) and (33), the background kinetic term and its perturbation can be written as

$$\begin{aligned}\bar{X} &= \frac{(\bar{\phi}')^2}{2a^2} \\ \delta X_{\bar{h}} &= \bar{X}(\Phi + 3\Psi)\end{aligned}\quad (34)$$

where a prime denotes differentiation with respect to conformal time,  $' \equiv \partial_{\eta}$ .

Substituting Eqs. (33) and (34) into Eq. (25), we obtain the nonvanishing components of  $M_{\mu\nu}(\tilde{h})$  as

$$\begin{aligned}M_{00}(\tilde{h}) &= 2a^2\Phi\left[\mathcal{L} + \bar{X}\mathcal{L}_X + 2\bar{X}^2\mathcal{L}_{XX}\right] \\ M_{ij}(\tilde{h}) &= 2a^2\left[\mathcal{L}\Psi - \bar{X}\mathcal{L}_X\Phi\right]\delta_{ij} - \frac{a^2}{2}\mathcal{L}h_{ij}^{(TT)}\end{aligned}\quad (35)$$

Similarly, inserting the nonzero background curvature tensors listed in Appendix B into Eq. (28), we obtain the nonvanishing components of the curvature contribution  $\tilde{W}_{\mu\nu}$  appearing in Eq. (27) as

$$\begin{aligned}\tilde{W}_{00} &= 3\mathcal{H}'[3\Psi - \Phi] + 12\mathcal{H}^2\Psi \\ \tilde{W}_{ij} &= \delta_{ij}\left[\mathcal{H}'(7\Psi - 5\Phi) - 6\mathcal{H}^2(\Phi - \Psi)\right] \\ &\quad + (2\mathcal{H}' + 3\mathcal{H}^2)h_{ij}^{(TT)},\end{aligned}\quad (36)$$

where  $\mathcal{H}$  is the conformal Hubble parameter, which can be defined as  $\mathcal{H} \equiv \left(\frac{a'}{a}\right)$ .

#### IV. MODIFIED GWS EQUATION THROUGH A NON-CANONICAL LAGRANGIAN

In this section, we derive the modified gravitational-wave equation for a particular choice of non-canonical Lagrangian and then rewrite it in terms of the redshift  $z$  for confronting the model with observations.

##### A. Form of Modified GWs Equation

Substituting Eqs. (33), (35), and (34) into Eq. (27), we obtain two independent components of the Einstein equations: the 00 component and the  $ij$  component. The 00 component together with the scalar part of the  $ij$  component describes the relation between the metric potentials  $\Phi$  and  $\Psi$  and governs their time evolution. By contrast, the tensor (transverse–traceless) part of the  $ij$  component corresponds to tensor perturbations, i.e., gravitational waves.

As discussed earlier, in the presence of a k-essence background the metric perturbations generically decompose into scalar, vector, and tensor sectors, with the scalar sector being sourced by the underlying scalar field and giving rise to additional, typically non-radiative modes. In contrast, the tensor sector—corresponding to the transverse–traceless (TT) part of the spatial metric perturbation—contains the true dynamical degrees of freedom associated with freely propagating gravitational waves [14, 34–38]. This separation follows from the gauge-invariant decomposition

of perturbations on a curved background, where only the TT tensor modes remain invariant under scalar and vector gauge transformations and satisfy a wave-like equation.

Physically, scalar and vector perturbations are either constrained by the field equations or decay with the cosmological expansion, and hence do not represent propagating radiative degrees of freedom. By contrast, the TT tensor modes propagate causally and carry energy and information across spacetime, making them the relevant observables for gravitational-wave physics. Therefore, to extract the physical propagation equation for gravitational waves from the perturbed Einstein equations, it is necessary and sufficient to project onto the TT sector of the spatial perturbations. This is achieved by applying the transverse–traceless projection operator, which systematically removes the non-dynamical (longitudinal and trace) components and isolates the tensor mode  $h_{ij}^{(TT)}$  [14, 15, 34].

In the context of k-essence or more general modified-gravity scenarios, this procedure is particularly important because the scalar-field background can source additional metric perturbations that mix with the scalar sector but do not correspond to propagating gravitational radiation. The TT projection ensures that such non-radiative contributions are excluded, leaving a closed evolution equation for  $h_{ij}^{(TT)}$  that captures the modified propagation of gravitational waves in the given background. Consequently, the dynamics of  $h_{ij}^{(TT)}$  encodes the physically observable gravitational-wave signal, including possible deviations from general relativity induced by the k-essence field.

Accordingly, to obtain the gravitational-wave sector from the  $ij$  component, we retain only the TT-surviving parts of  $\tilde{h}_{ij}$ ,  $\tilde{W}_{ij}$ , and  $M_{ij}(\tilde{h})$  in Eqs. (33), (35), and (36), respectively. Acting with the TT projector [14, 15, 34] then yields

$$\begin{aligned}\tilde{h}_{ij}^{TT} &= -\frac{a^2}{2}h_{ij}^{(TT)} \\ \tilde{W}_{ij}^{TT} &= (2\mathcal{H}' + 3\mathcal{H}^2)h_{ij}^{(TT)} \\ M_{ij}^{TT}(\tilde{h}) &= -\frac{a^2}{2}\mathcal{L}h_{ij}^{(TT)}\end{aligned}\quad (37)$$

Under the TT projection, the  $ij$  component of the Einstein equations reduces to

$$\boxed{-\frac{1}{2}\bar{\square}\tilde{h}_{ij}^{TT} + \tilde{W}_{ij}^{TT} = 8\pi GM_{ij}^{TT}(\tilde{h})}\quad (38)$$

Substituting Eq. (37) into Eq. (38), we obtain

$$\begin{aligned}\frac{1}{4}\bar{\square}(a^2h_{ij}^{(TT)}) + (2\mathcal{H}' + 3\mathcal{H}^2)h_{ij}^{(TT)} \\ + 4\pi Ga^2h_{ij}^{(TT)}\mathcal{L}(\bar{X}, \bar{\phi}) = 0\end{aligned}\quad (39)$$

Applying the background d'Alembertian  $\bar{\square} = \bar{g}^{\mu\nu}\bar{\nabla}_\mu\bar{\nabla}_\nu$  in the TT ( $ij$ ) sector, we obtain the simplified gravitational-wave equation as follows:

$$\begin{aligned}h_{ij}^{(TT)''} + 2\mathcal{H}h_{ij}^{(TT)'} - \nabla^2h_{ij}^{(TT)} \\ + \left[8\mathcal{H}' + 10\mathcal{H}^2 + 16\pi Ga^2\mathcal{L}(\bar{X}, \bar{\phi})\right]h_{ij}^{(TT)} = 0\end{aligned}\quad (40)$$

Equation (40) is *the modified gravitational-wave equation in the transverse-traceless (TT) sector*, which is obtained in our setup, which deviates from the standard GR result [14]. The last term in Eq. (40) acts as an effective mass-like contribution proportional to  $h_{ij}^{(TT)}$ , sourced by the curvature term  $\tilde{W}_{ij}^{TT}$  and the k-essence Lagrangian.

## B. Specific Choice of Non-Canonical Lagrangian

We now consider a specific choice of the non-canonical k-essence Lagrangian  $\mathcal{L}(X, \phi)$  for our gravitational-wave analysis.

For the k-essence scalar field  $\phi$ , the pressure  $P_\phi$ , energy density  $\rho_\phi$ , equation-of-state (EoS) parameter  $w_\phi$ , and sound speed  $c_s^2$  are given, respectively, by [28, 40–48]

$$\begin{aligned} P_\phi &= \mathcal{L}(X, \phi) \\ \rho_\phi &= 2X\mathcal{L}_X - \mathcal{L} \\ w_\phi &= \left(\frac{P}{\rho}\right) = \frac{\mathcal{L}(X, \phi)}{2X\mathcal{L}_X - \mathcal{L}} \\ c_s^2 &= \frac{(\partial P/\partial X)}{(\partial \rho/\partial X)} = \frac{\mathcal{L}_X}{2X\mathcal{L}_{XX} + \mathcal{L}_X}. \end{aligned} \quad (41)$$

From Eq. (41), we obtain a differential equation relating the sound speed  $c_s^2$  to the Lagrangian  $\mathcal{L}(X, \phi)$  (for  $c_s^2 \neq 0$ ):

$$2X\mathcal{L}_{XX} - \left(\frac{1 - c_s^2}{c_s^2}\right)\mathcal{L}_X = 0 \quad (42)$$

Therefore, the general solution of Eq. (42) is given by [63–65]:

$$\mathcal{L}(X, \phi) = U(\phi)X^n - V(\phi) \quad (43)$$

where  $U(\phi)$  and  $V(\phi)$  are arbitrary functions of  $\phi$ , and  $n = (1 + c_s^2)/(2c_s^2)$  is a constant.

For simplicity, we set  $U(\phi) = 1$ , in which case the Lagrangian takes the form [66]

$$\mathcal{L}(X, \phi) = X^n - V(\phi). \quad (44)$$

This is the specific non-canonical k-essence Lagrangian adopted in our gravitational-wave analysis.

Here  $V(\phi)$  plays the role of the potential for the scalar field  $\phi$ . Substituting Eq. (44) into Eq. (41), we obtain

$$\begin{aligned} P_\phi &= X^n - V(\phi), \\ \rho_\phi &= (2n - 1)X^n + V(\phi), \\ c_s^2 &= \frac{1}{2n - 1} = \text{constant}. \end{aligned} \quad (45)$$

The sound speed must satisfy  $0 < c_s^2 \leq 1$ , which implies  $n \geq 1$  [63, 64, 66]. From Eq. (45), one finds  $c_s^2 = 1$  for  $n = 1$  (the quintessence limit), while for  $n > 1$  the sound speed decreases monotonically from unity as  $n$  increases [66]. An important aspect of non-canonical scalar-field theories is the theoretical consistency of the perturbative sector: viable k-essence cosmologies must

be free from both ghost and gradient instabilities. The no-ghost condition requires  $\mathcal{L}_X > 0$  [67–70], which guarantees that the coefficient associated with the scalar perturbations proportional to  $X\mathcal{L}_X/H^2$  do not carry negative kinetic energy [67]. The absence of Laplacian instabilities further requires  $c_s^2 > 0$  [67]. For the power-law kinetic structure considered here,  $c_s^2 = 1/(2n - 1)$ , so stability is automatically satisfied for  $n > 1/2$ , while enforcing subluminal propagation,  $c_s^2 \leq 1$ , restricts the model to the physically relevant regime analyzed in this work.

Accordingly, the parameter region used in our observational analysis satisfies these stability conditions throughout the relevant stages of cosmic evolution. Moreover, since the tensor propagation speed remains exactly luminal,  $c_{\text{gw}} = 1$ , the model naturally evades the stringent multimessenger constraints from GW170817 [16]. In this framework, the non-canonical kinetic sector primarily affects the dispersive properties of gravitational-wave propagation through the effective tensor mass term, while preserving the causal structure and stability of the underlying theory.

For a homogeneous background in conformal time, the non-canonical k-essence Lagrangian becomes  $\mathcal{L}(\bar{X}, \bar{\phi}) = \left(\frac{\bar{\phi}^2}{2a^2}\right)^n - V(\bar{\phi})$ . The corresponding background energy density  $\bar{\rho}_\phi$ , pressure  $\bar{P}_\phi$ , and equation-of-state parameter  $\bar{w}_\phi$  then follow from Eq. (45):

$$\begin{aligned} \bar{\rho}_\phi &= (2n - 1)\bar{X}^n + V(\bar{\phi}) \\ \bar{P}_\phi &= \bar{X}^n - V(\bar{\phi}) \\ \bar{w}_\phi &= \left(\frac{\bar{P}_\phi}{\bar{\rho}_\phi}\right) = \frac{\bar{X}^n - V(\bar{\phi})}{(2n - 1)\bar{X}^n + V(\bar{\phi})} \end{aligned} \quad (46)$$

Thus, at linear order, the gravitational-wave equation (40) can be written as

$$\boxed{h_{ij}^{(TT)''} + 2\mathcal{H}h_{ij}^{(TT)'} - \nabla^2 h_{ij}^{(TT)} + m_{\text{eff}}^2 h_{ij}^{(TT)} = 0} \quad (47)$$

where

$$m_{\text{eff}}^2 \equiv 8\mathcal{H}' + 10\mathcal{H}^2 + 16\pi G a^2 \mathcal{L}(\bar{X}, \bar{\phi}) \quad (48)$$

defines an effective mass-squared (i.e., potential) term for the tensor mode, encoding background-field corrections to gravitational-wave propagation from both the cosmological expansion and the background k-essence Lagrangian.

Using the conformal-time background Friedmann equations (Appendix B), assuming a pressureless (dust) background, and employing the definitions in Eq. (46), the effective-mass term  $m_{\text{eff}}^2$  (48) simplifies to

$$\begin{aligned} m_{\text{eff}}^2 &= 16\pi G a^2 (\eta)(\bar{\rho} - \bar{P}) \\ \text{or, } m_{\text{eff}}^2 &= 16\pi G a^2 (\eta)[(1 - \bar{w}_\phi)\bar{\rho}_\phi + \bar{\rho}_m] \end{aligned} \quad (49)$$

It is important to clarify the physical interpretation of the term  $m_{\text{eff}}^2$  appearing in Eq. (49). This contribution should not be understood as a fundamental rest mass for the graviton: the propagating degree of freedom is still the standard massless spin-2 tensor mode

of general relativity, with two transverse polarizations and luminal propagation speed,  $c_{\text{gw}} = 1$ . Instead,  $m_{\text{eff}}^2$  arises as a background-induced, time-dependent modification of the tensor wave equation, generated by the interaction of tensor perturbations with the evolving cosmological background sourced by the k-essence Lagrangian  $\mathcal{L}(\bar{X}, \bar{\phi})$ . In this sense,  $m_{\text{eff}}^2$  acts as an effective mass-like (dispersive) term that modifies the dispersion relation without introducing additional tensor degrees of freedom or altering the causal structure of the theory. To avoid confusion with a genuine massive-gravity scenario (e.g. Fierz-Pauli or dRGT), we emphasize that this term does not correspond to a fundamental graviton mass. Rather, it encodes medium-like effects induced by cosmological background leading to a frequency-dependent phase shift accumulated during propagation over cosmological distances. This behavior is analogous to electromagnetic waves in a plasma, where an effective mass emerges from medium effects without implying a true photon mass [87–89].

We now write the Fourier transform of the tensor perturbation  $h_{ij}^{(TT)}$  as [14, 34, 59, 71]:

$$h_{ij}^{(TT)}(\eta, \mathbf{x}) = \sum_{A=+, \times} \int \frac{d^3k}{(2\pi)^{\frac{3}{2}}} h_A(\eta, \mathbf{k}) e_{ij}^{(A)}(\mathbf{k}) e^{i\mathbf{k}\cdot\mathbf{x}} \quad (50)$$

where  $h_A(\eta, \mathbf{k})$  denotes the Fourier mode of the gravitational-wave amplitude,  $\mathbf{k}$  is the comoving wavevector, and  $e_{ij}^{(A)}(\mathbf{k})$  is the (symmetric) transverse-traceless polarization tensor [59]. The index  $A$  labels the two polarization states,  $A = +, \times$ , and  $e^{i\mathbf{k}\cdot\mathbf{x}}$  denotes the plane-wave basis. We emphasize that the normal-mode (Fourier) expansion introduced in Eqs. (50) and (54) is a purely classical decomposition of the linearized field and does not entail any quantization of gravity. It is simply the standard plane-wave expansion of metric perturbations into independent modes labeled by the comoving wavevector  $\mathbf{k}$  and polarization tensors, widely used to solve linear partial differential equations in classical field theory [34, 97, 98, 124]. Accordingly, the mode functions  $h_A(\eta, \mathbf{k})$  (or  $\chi_A$ ) are ordinary complex-valued amplitudes of classical gravitational waves, and in the linear regime each mode evolves independently on the prescribed background spacetime. No quantum structure is introduced: the expansion coefficients are not promoted to operators and no commutation relations are imposed, unlike in a quantum-field-theoretic treatment where one introduces creation and annihilation operators [99]. The procedure is therefore directly analogous to the classical Fourier decomposition of electromagnetic or acoustic waves and should be understood solely as a tool for analyzing gravitational-wave propagation in a cosmological background.

Substituting Eq. (50) into Eq. (47), we obtain the modified linearized gravitational-wave equation

in Fourier space:

$$\boxed{h''_A + 2\mathcal{H}h'_A + (k^2 + m_{\text{eff}}^2)h_A = 0} \quad (51)$$

Equation (51) is the modified GW propagation equation for tensor perturbations in a k-essence scalar-field background. Throughout this work, we assume a homogeneous scalar configuration,  $\phi = \bar{\phi}(\eta)$ ; in unitary gauge, one sets  $\delta\phi = 0$ , so the scalar perturbation does not enter the tensor sector at linear order [55, 57, 58, 72]. Gravitational waves, therefore, propagate purely as metric tensor perturbations [14, 15, 34, 54], while the k-essence field affects their evolution only through background quantities that appear in the effective mass term  $m_{\text{eff}}^2$ . In particular,  $m_{\text{eff}}^2$  receives contributions from both the background expansion and the background k-essence Lagrangian  $\mathcal{L}(\bar{X}, \bar{\phi})$ , implying that the scalar field modifies GW propagation indirectly through the effective spacetime geometry. Hence, at linear order the k-essence field alters the GW evolution and dispersion without providing an independent tensor-source term. Equation (51) follows after consistently fixing the gauge freedom so as to isolate the physical tensor degrees of freedom. For the background and scalar sector we work in the conformal Newtonian (longitudinal) gauge, which removes the scalar shift and shear and cleanly separates scalar and tensor perturbations. We then impose the transverse-traceless (TT) conditions on the spatial metric perturbation,  $\partial^i h_{ij} = 0$  and  $h^i_i = 0$ , thereby isolating the two propagating gravitational-wave polarizations. In addition, we adopt unitary gauge ( $\delta\phi = 0$ ), so that scalar-field fluctuations are absorbed into the background and do not contribute to the tensor dynamics at linear order. Equation (51) is therefore the fully gauge-fixed evolution equation for the physical gravitational-wave amplitudes  $h_{ij}^{(TT)}$  on a conformal-Newtonian background.

We note, however, that even if one retained the scalar-field perturbation, it would not directly modify the tensor evolution equation at linear order. In first-order cosmological perturbation theory the scalar, vector, and tensor sectors evolve independently, and a minimally coupled scalar field does not generate anisotropic stress that can source transverse-traceless metric perturbations. Accordingly, the tensor mode  $h_{ij}^{(TT)}$  evolves independently of the scalar fluctuation  $\delta\phi$  in the linear regime. The k-essence influence on GW propagation therefore enters only through background quantities—such as the scale factor and the homogeneous field configuration  $\bar{\phi}(\eta)$  in conformal time—which contribute to the effective mass term  $m_{\text{eff}}^2$  in Eq. (51). A direct coupling between  $\delta\phi$  and tensor modes would arise only beyond linear order, or in theories where the scalar sector produces anisotropic stress.

We now discuss the propagation speed of gravitational waves. In effective-field-theory (EFT) approaches to late-time cosmology—in particular the EFT of dark energy/modified gravity—the quadratic action for tensor modes can be written schematically as  $S_T \sim \int d\eta d^3x a^2 [Q_T (h'_{ij})^2 - c_{gw}^2 (\partial_k h_{ij})^2]$ , so that

the coefficient of the  $k^2$  term in the tensor equation of motion directly defines the GW propagation speed  $c_{gw}$  [57, 72, 73, 75, 76]. Therefore, any departure from unity in front of  $k^2$  in Eq. (51) would correspond to  $c_{gw} \neq c$ . The joint observation of the binary neutron-star merger GW170817 [16] and the associated gamma-ray burst GRB 170817A [17] imposes a remarkably tight bound on this deviation,  $|c_{gw} - c|/c \lesssim 10^{-15}$ , thereby excluding large classes of scalar–tensor and vector–tensor modifications of GR and strongly restricting EFT operators that predict  $c_{gw} \neq 1$  [24–26, 77].

However, our model automatically satisfies these bounds because the  $k$ -essence field is minimally coupled and the Lagrangian takes the form  $\mathcal{L}(X, \phi) = X^n - V(\phi)$ . In this case, the tensor sector retains the standard gradient term, so the coefficient of  $k^2$  in Eq. (51) remains unity and the GW speed is luminal,  $c_{gw}^2 = 1$ . The only modification to GW propagation in our setup is therefore dispersive: it enters through the effective mass term  $m_{\text{eff}}^2$ , rather than through a change in the fundamental propagation speed.

In Eq. (51), the term  $2\mathcal{H}h'_A$  acts as a Hubble-friction term induced by the cosmic expansion, where the conformal Hubble parameter is  $\mathcal{H} \equiv a'/a$ . For GW propagation on an expanding FLRW background it is often convenient to absorb this damping by redefining the tensor amplitude, thereby eliminating the first-derivative term from the mode equation.

In this context, we introduce an auxiliary (rescaled) tensor mode  $\chi_A(\eta, \mathbf{k})$  via [18, 78]

$$h_A(\eta, \mathbf{k}) = \frac{1}{a(\eta)} \chi_A(\eta, \mathbf{k}), \quad (52)$$

where the factor  $1/a(\eta)$  accounts for the cosmological dilution of the GW amplitude during propagation. With this field redefinition, the Hubble-friction term  $2\mathcal{H}h'_A$  in Eq. (51) is absorbed into the evolution equation for  $\chi_A(\eta, \mathbf{k})$ , yielding a second-order mode equation without a first-derivative (damping) term [18, 78].

By introducing this variable  $\chi_A(\eta, \mathbf{k})$ , Eq.(51) becomes,

$$\chi''_A + \left(k^2 + m_{\text{eff}}^2 - \frac{a''}{a}\right) \chi_A = 0 \quad (53)$$

Thus, the rescaling (52) removes the first-derivative (Hubble-friction) term  $2\mathcal{H}h'_A$  in Eq. (51) and casts the tensor-mode dynamics into a simpler second-order equation (53) for  $\chi_A$ , with an effective time-dependent potential  $a''/a$  and the additional dispersive contribution from the effective mass term  $m_{\text{eff}}^2$ . This form is often more transparent for physical interpretation and analytic estimates of GW propagation on an expanding background.

We now introduce the high-frequency (short-wavelength) approximation known as the *sub-horizon* or *sub-Hubble* limit [18, 34, 54, 78]. In this regime the physical wavelength of the perturbation is much smaller than the horizon scale, i.e.  $\lambda_{\text{phys}} \ll R_H$ , where

$R_H \equiv a/\mathcal{H}$  is the (comoving) Hubble radius. For tensor perturbations in an FLRW background, this limit considerably simplifies the evolution equation and is particularly useful for studying gravitational-wave propagation over cosmological distances. It isolates the genuine wave dynamics from the large-scale expansion effects that dominate on super-horizon scales [34], where perturbations effectively freeze, and thus provides a natural arena to test possible modifications of general relativity.

For sub-horizon modes, we have  $k\eta \gg 1$ . Moreover, during both the matter-dominated era and the late-time dark-energy-dominated epoch, the quantity  $a''/a$  is of order  $\eta^{-2}$  (up to factors of order unity) [18, 34, 54, 78]. Hence, in the sub-horizon regime one typically has  $k^2 \gg a''/a$ , and the term  $a''/a$  in Eq. (53) can be neglected compared to  $k^2$ .

Therefore, within this approximation, Eq. (53) reduces to

$$\chi''_A + \left(k^2 + m_{\text{eff}}^2\right) \chi_A = 0, \quad (54)$$

which is a modified propagation equation for the GW modes in a non-trivial cosmological background.

The derivation of the modified gravitational-wave propagation equation (54) relies on the standard short-wavelength (sub-horizon) approximation, i.e. tensor modes evolve well inside the Hubble horizon. In this regime, the GW wavelength is much smaller than the characteristic curvature scale of the cosmological background, so tensor perturbations propagate approximately as free waves on a slowly varying space-time. This approximation is well suited to the observational bands of current ground-based detectors such as LIGO/Virgo/KAGRA, with typical frequencies  $f \sim \mathcal{O}(10\text{--}10^3)$  Hz, and to future space-based missions such as LISA, operating around  $f \sim \mathcal{O}(10^{-4}\text{--}10^{-1})$  Hz. For these frequencies, the physical wavelength remains much smaller than the Hubble radius ( $\sim 1/H$ ) during most of the propagation history, consistently justifying the sub-horizon limit adopted here,  $k^2 \gg a''/a$ .

For ultra-low-frequency signals, such as those targeted by pulsar timing arrays, or for primordial tensor modes near horizon crossing, the approximation can break down and long-wavelength corrections (including the  $a''/a$  term and other background-curvature contributions) may become important. Accordingly, the dispersive corrections derived in this section should be interpreted as describing the propagation of sub-horizon astrophysical gravitational waves rather than super-horizon primordial tensor perturbations.

In standard general relativity, the corresponding equation,  $\chi''_A + k^2\chi_A = 0$  [18, 78], describes freely propagating massless tensor perturbations with a linear dispersion relation  $\omega = k$  [78]. The extra term  $m_{\text{eff}}^2$  in Eq. (54) acts as an effective (time-dependent) contribution to the wave dynamics—originating from the coupling between tensor perturbations and the background  $k$ -essence scalar field  $\bar{\phi}$ , as well as from the background expansion—and therefore modifies the dispersion relation. As a consequence, different Fourier modes accumulate different phases during propagation,

producing a frequency-dependent phase shift absent in standard GR. This effect can, in principle, be exploited observationally to probe the properties of dark energy through GW measurements.

Accordingly, Eq. (54) implies the modified dispersion relation  $\omega_{\text{eff}}^2 = k^2 + m_{\text{eff}}^2$ , where  $\omega_{\text{eff}}$  differs from the standard  $\omega$  due to the presence of  $m_{\text{eff}}$  term. As discussed earlier  $m_{\text{eff}}$  does not represent a fundamental graviton mass; rather, it acts as an effective potential term for the tensor modes, encoding background-field corrections to gravitational-wave propagation arising from both the cosmological expansion and the underlying k-essence Lagrangian. In the high-frequency limit  $k^2 \gg |m_{\text{eff}}^2|$  one may expand  $\omega_{\text{eff}} \simeq k(1 + \frac{m_{\text{eff}}^2}{2k^2})$ . Thus, the cumulative phase shift  $\Delta\Theta$  acquired during propagation can be written as

$$|\Delta\Theta| = \int \frac{m_{\text{eff}}^2}{2k} d\eta. \quad (55)$$

Although the GW propagation speed remains equal to the speed of light—as ensured by the unmodified coefficient of the  $k^2$  term in Eq. (51)—the presence of the  $m_{\text{eff}}^2$  term induces a non-trivial dispersion relation. This, in turn, leads to a frequency-dependent modification of GW propagation and hence to cumulative phase shifts over cosmological distances.

An important feature of the modified gravitational-wave propagation considered in this framework is the potential observational signature associated with the cumulative phase correction given by the effective tensor mass term. Although the quantity  $m_{\text{eff}}$  remains relatively small (an ultra-light physical scale) throughout the cosmological evolution, its contribution to the gravitational-wave phase may accumulate over very large propagation distances, potentially generating observable dispersive signatures in the detected waveform. In this form, the cumulative phase shift introduced in Eq. (55) depends both on the cosmological background evolution and on the wavelength of the propagating tensor mode, implying that long-wavelength gravitational waves traveling across cosmological distances may be especially sensitive to these corrections.

In this context, the dispersive contribution associated with  $m_{\text{eff}}$  may lead to small but non-negligible modifications in the phase evolution of gravitational-wave signals compared with the standard prediction of general relativity, since the correction accumulates continuously during propagation. Moreover, the phase correction generated by the effective tensor mass differs qualitatively from a simple modification of the waveform amplitude, since it introduces a frequency-dependent propagation effect associated with the cosmological background itself. This feature could, in principle, allow future GW observations to distinguish the present scenario from standard general relativity through precision analyses of waveform propagation over cosmological distances.

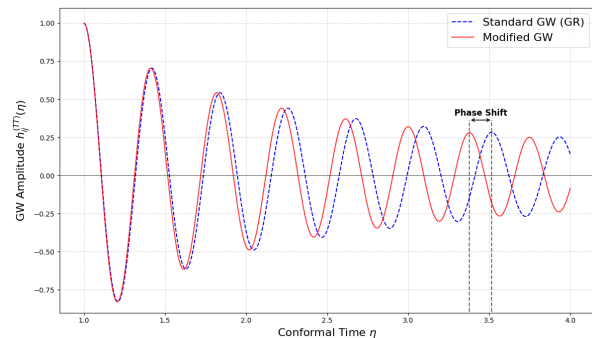


Figure 1: Comparison of the transverse–traceless gravitational-wave amplitude  $h_{ij}^{(\text{TT})}$  as a function of conformal time  $\eta$ . The dashed blue curve shows the standard massless propagation in GR, while the solid red curve shows the modified propagation in the k-essence framework. The k-essence waveform accumulates a progressive phase shift relative to the GR prediction.

Figure (1) shows the evolution of the gravitational-wave amplitude as a function of conformal time  $\eta$ , comparing the standard GR prediction with the modified propagation in the k-essence framework. Although both waveforms display the expected  $1/a$  damping from the cosmological expansion, the k-essence signal (solid red line) progressively dephases relative to the massless GR case (dashed blue line). This cumulative phase shift arises from the effective mass term  $m_{\text{eff}}^2$  in the Fourier-mode evolution equation (51), which alters the dispersion relation through the interaction with the background k-essence field. For a dynamical background described by the Lagrangian  $\mathcal{L} = X^n - V(\phi)$ , the nonzero  $m_{\text{eff}}^2$  leads to frequency-dependent propagation, producing the late-time phase variation seen in the figure (Fig. 1).

A more detailed numerical study, including realistic waveform templates and detector sensitivities, would be necessary in order to quantify the precise observational detectability of the predicted dispersive effects. Such an analysis lies beyond the scope of the present work and will be explored in future investigations. In addition, future high-precision gravitational-wave observations could provide an important observational window into the cosmological dynamics of the underlying k-essence sector. In particular, observations involving sources located at high redshifts may enhance the cumulative effect and therefore improve the possibility of constraining the effective tensor mass evolution.

Before proceeding further, we clarify the scope of field interactions considered in this work. In astrophysical environments—such as core-collapse supernovae [79] and compact binary systems [80]—gravitational waves can couple to electromagnetic and acoustic fields and may generate secondary radiation [81–85]. Such effects are typically associated with media that support anisotropic stresses and/or nonlinear couplings [86]. Here, by contrast, we study the linear propaga-

tion of transverse–traceless tensor perturbations on a homogeneous and isotropic FLRW background sourced by a minimally coupled k-essence scalar field. In linear cosmological perturbation theory, the scalar, vector, and tensor sectors evolve independently [98, 124], and at first order the tensor modes are not sourced by electromagnetic or scalar perturbations. In particular, for a homogeneous cosmological background one has  $\langle F_{\mu\nu} \rangle = 0$ , so no electromagnetic anisotropic stress is generated to couple to the tensor sector. Gravitational waves therefore propagate as free tensor modes, with their dynamics modified only through background quantities entering the effective field equations.

On cosmological scales, and within the high-frequency (sub-horizon) approximation adopted here, the decoupling of the radiative tensor sector from scalar and vector perturbations is well justified. In this regime, the leading modification to gravitational-wave propagation is controlled by the time-dependent k-essence background and is conveniently encoded in a redshift-dependent effective mass term. While electromagnetic mixing may be relevant in localized astrophysical events, its contribution to the large-scale, linear propagation of cosmological GWs is expected to be negligible compared to the geometric effects induced by the dark-sector background.

Accordingly, our goal is to isolate the impact of the k-essence dark sector on the gravitational-wave dispersion relation within a minimal and controlled setup. Extensions that include electromagnetic fields, non-minimal couplings, or higher-order perturbative effects could introduce additional mixing phenomena and are an interesting direction for future work, but are beyond the scope of the present analysis.

### C. Formulations in Redshift ( $z$ ) Space

In this subsection, we transform the dependence of the effective mass term  $m_{\text{eff}}^2$  in Eq. (49) from conformal time  $\eta$  to redshift  $z$ .

We use the following relations [18, 34, 54, 78]:

$$\begin{aligned} \frac{a(\eta)}{a_0} &= \frac{1}{1+z} \\ \mathcal{H} &= -\frac{1}{1+z} \frac{dz}{d\eta} \end{aligned} \quad (56)$$

where  $a_0$  is the present value of the scale factor.

At late times, the contribution of radiation is negligible compared to that of dark matter and dark energy [90]. Therefore, imposing covariant conservation of the total background energy–momentum tensor (see Appendix B, Eq. (B10)),  $\bar{\nabla}_\mu \bar{T}^{\mu\nu} = 0$ , we obtain the following continuity equations:

$$\begin{aligned} \bar{\rho}'_\phi + 3\mathcal{H}(\bar{\rho}_\phi + \bar{P}_\phi) &= 0 \\ \bar{\rho}'_m + 3\mathcal{H}(\bar{\rho}_m + \bar{P}_m) &= 0 \end{aligned} \quad (57)$$

If the background scalar field  $\bar{\phi}$  accounts for the dark-energy sector, we may identify  $\Omega_\phi \equiv \Omega_{\text{de}}$  and  $w_\phi \equiv w_{\text{de}}$ , where  $\Omega_{\text{de}}$  and  $w_{\text{de}}$  denote the dark-energy

density parameter and equation-of-state (EoS) parameter, respectively [54, 90]. In the standard  $\Lambda$ CDM model, dark energy is a cosmological constant  $\Lambda$  with fixed EoS  $w_{\text{de}} = -1$ . A widely used minimal extension is the  $w$ CDM model, in which the dark-energy EoS is promoted to a constant free parameter  $w_{\text{de}} \neq -1$ . More general phenomenological extensions allow a redshift-dependent EoS, e.g. the CPL form  $w(z) = w_0 + w_a z/(1+z)$  [91, 92]. In our notation, this corresponds to a  $w_\phi$ CDM description.

Cold dark matter is non-relativistic at late times, with a tiny velocity dispersion, so its background pressure is negligible compared to its energy density,  $\bar{P}_m \simeq 0$  (i.e.  $w_m \equiv \bar{P}_m/\bar{\rho}_m \approx 0$ ), and the matter sector can be treated as dust [54] (considering for our case). With  $\bar{P}_m = 0$ , Eq. (57) yields

$$\begin{aligned} \bar{\rho}_m(z) &= \bar{\rho}_{m,0}(1+z)^3, \\ \bar{\rho}_\phi(z) &= \bar{\rho}_{\phi,0}(1+z)^{3(1+w_\phi)} \end{aligned} \quad (58)$$

where  $\bar{\rho}_{\phi,0}$  and  $\bar{\rho}_{m,0}$  are the present-day energy densities of the scalar field and matter, respectively.

Using Eqs. (49) and (58), we can now express  $m_{\text{eff}}^2$  as a function of redshift  $z$  as

$$\begin{aligned} m_{\text{eff}}^2(z) &= \frac{6H^2}{(1+z)^2} \left[ (1 - \bar{w}_\phi)\Omega_\phi + \Omega_m \right] \\ \text{or,} \\ m_{\text{eff}}^2(z) &= \frac{6H_0^2}{(1+z)^2} \left[ (1 + \bar{w}_\phi)\Omega_{\phi,0}(1+z)^{3(1+\bar{w}_\phi)} \right. \\ &\quad \left. + \Omega_{m,0}(1+z)^3 \right] \end{aligned} \quad (59)$$

where  $H_0$  is the present day Hubble constant,  $\Omega_\phi \equiv \frac{\kappa^2 \bar{\rho}_\phi}{3H^2}$  and  $\Omega_m \equiv \frac{\kappa^2 \bar{\rho}_m}{3H^2}$  are energy density parameter for the scalar field and the matter respectively, on the other hand,  $\Omega_{\phi,0} \equiv \frac{\kappa^2 \bar{\rho}_{\phi,0}}{3H_0^2}$  and  $\Omega_{m,0} \equiv \frac{\kappa^2 \bar{\rho}_{m,0}}{3H_0^2}$  are the present day energy density parameter for the scalar field and the matter respectively. We have also used the relation between the conformal Hubble parameter  $\mathcal{H}$  and the standard or physical Hubble parameter  $H$ , i.e.  $\mathcal{H} = aH$ , with the scale factor  $a = \frac{1}{(1+z)}$ .

Equation (59) makes explicit that the effective mass  $m_{\text{eff}}^2$  governing tensor-mode propagation is sourced by the background cosmological fluid. In particular, through Eq. (49),  $m_{\text{eff}}^2$  depends on the scalar-field energy density  $\bar{\rho}_\phi$  and pressure  $\bar{P}_\phi$ , as obtained from the linearized field equations in Eq. (40). The dependence on the scalar-field EoS parameter  $\bar{w}_\phi$  in Eqs. (49) and (59) implies that different dark-energy realizations—and, in our case, different choices of non-canonical Lagrangians  $\mathcal{L}(X, \phi)$ —lead to distinct modifications of the tensor dispersion relation. Moreover, the explicit redshift dependence of  $m_{\text{eff}}^2(z)$  in Eq. (59) shows that the modification is dynamical, with different cosmological epochs (matter or dark-energy dominated) contributing differently. Consequently, this time-dependent dispersion accumulates along the line of sight and can induce a cumulative phase shift for gravitational waves propagating over cosmological distances.

We now discuss the gravitational-wave luminosity distance  $D_L^{\text{GW}}(z)$ . In an FLRW spacetime, photons and gravitons propagate on the same background geometry, and in GR both follow null geodesics; consequently, the luminosity distance  $D_L(z)$  is determined solely by the expansion history. In many modified-gravity scenarios, a mismatch between  $D_L^{\text{GW}}$  and the electromagnetic luminosity distance  $D_L^{\text{EM}}$  can arise if the GW propagation speed differs from unity,  $c_{\text{gw}} \neq 1$ , and/or if an anomalous friction term changes the amplitude damping during propagation [18, 78]. In our case, Eqs. (47) and (51) show that the coefficient of friction term  $h'_A(\eta, \mathbf{k})$  remains exactly  $2\mathcal{H}$  and the propagation speed is luminal,  $c_{\text{gw}} = 1$ , so the GW amplitude decays as  $h_A \propto a^{-1}$ , exactly as in GR. Although the k-essence background induces the effective mass term  $m_{\text{eff}}^2$  in Eqs. (47) and (51), it modifies only the dispersion relation (phase/frequency evolution) and does not affect the amplitude damping. Therefore, in this framework, we have  $D_L^{\text{GW}}(z) = D_L^{\text{EM}}(z)$ , and we may define

$$D_L^{\text{GW}}(z) = c(1+z) \int_0^z \frac{dz_1}{H(z_1)} \quad (60)$$

where  $c$  is the speed of light in unit of  $km/s$ . Now taking the derivative concerning  $z$  in Eq. (60), we can get the following differential equation:

$$\frac{dD_L^{\text{GW}}(z)}{dz} = \frac{D_L^{\text{GW}}(z)}{(1+z)} + \frac{c(1+z)}{H(z)}. \quad (61)$$

Neglecting the radiation component at late times, and assuming a spatially flat universe, we have  $\Omega_\phi(z) + \Omega_m(z) = 1$ . Using this condition in the Friedmann equation (Appendix B, Eq. (B11)), the evolution of the Hubble parameter can be written as

$$\frac{dH}{dz} = \frac{3H(z)}{2(1+z)} \left[ 1 + w_\phi(z) \Omega_\phi(z) \right]. \quad (62)$$

Here we use the redshift-conformal-time relation  $dz/d\eta = -aH$  and, with the convention  $a_0 = 1$  (so  $a = 1/(1+z)$ ), this reduces to  $dz/d\eta = -H(z)$ .

The evolution of the scalar-field density parameter  $\Omega_\phi$  follows from its definition together with the continuity equations, and can be written as

$$\frac{d\Omega_\phi}{dz} = \frac{3\Omega_\phi}{1+z} (1 + w_\phi) - \frac{2\Omega_\phi}{H} \frac{dH}{dz}. \quad (63)$$

Combining Eqs. (62) and (63) gives the equivalent compact form

$$\frac{d\Omega_\phi}{dz} = \frac{3w_\phi(z)}{1+z} \Omega_\phi (1 - \Omega_\phi), \quad (64)$$

which is convenient for numerical integration.

#### D. Evolution Equation for the Scalar Field Model

Several cosmological studies have explored non-canonical scalar-field Lagrangians with a non-vanishing potential. In particular, Refs. [93–96] considered quadratic potentials in non-canonical frameworks, in

which the potential energy can play a central role in driving inflation in the early universe. For canonical scalar fields, a quadratic potential arises naturally from effective field theory considerations and has been widely employed in modeling inflation, dark energy, and dark matter.

In this work, we adopt the quadratic potential  $V(\bar{\phi}) = \frac{1}{2}m^2\bar{\phi}^2$  [93–96], where  $m$  is a free, positive, real parameter. This choice introduces a characteristic mass scale and leads to coherent oscillations of the field; depending on the kinetic structure of the model, the averaged dynamics may effectively behave as pressureless matter or yield accelerated expansion [100]. When combined with a non-trivial kinetic term, the setup remains analytically tractable while exhibiting rich dynamics, making it well-suited to explore the interplay between kinetic and potential contributions to cosmic evolution.

This quadratic potential ( $V(\phi)$ ) provides a simple and convenient framework for studying the evolution of the k-essence background together with the associated effects on gravitational-wave propagation. Nevertheless, the appearance of the effective tensor mass term is not exclusively tied to the quadratic form of  $V(\phi)$ . Rather, the modified dispersive behavior of gravitational waves originates primarily from the non-canonical kinetic structure of the k-essence sector and its coupling to the evolving cosmological background.

We therefore expect qualitatively similar gravitational-wave propagation effects to arise for other classes of scalar-field potentials, including exponential, inverse power-law, and plateau-type potentials commonly studied in dark-energy and inflationary scenarios. While the detailed redshift evolution of the effective tensor mass  $m_{\text{eff}}(z)$  will depend on the background dynamics associated with a given potential, the mechanism responsible for the frequency-dependent phase corrections remains the same, provided the non-canonical kinetic sector plays a non-negligible role in the cosmic evolution.

Different choices of  $V(\phi)$  can modify the late-time evolution of the Hubble parameter and the scalar-field energy density, thereby changing both the amplitude and the redshift dependence of the dispersive corrections in the gravitational-wave sector. Consequently, future analyses with alternative potentials may reveal additional phenomenological signatures and could improve the model's compatibility with cosmological observations. A detailed comparative study of different scalar-field potentials is left for future work.

Using the non-canonical Lagrangian  $\mathcal{L}(X, \phi)$  introduced in Eq. (44), the equation of motion (EoM) for the homogeneous background scalar field  $\bar{\phi}$  reads

$$\bar{\phi}'' + \frac{2(2-n)}{2n-1} \mathcal{H} \bar{\phi}' + \frac{2^{n-1}}{n(2n-1)} a^{2n} \bar{\phi}'^{(2-2n)} \left( \frac{dV}{d\bar{\phi}} \right) = 0 \quad (65)$$

where primes denote derivatives with respect to con-

formal time  $\eta$ . We introduce the field “velocity”

$$\begin{aligned}\bar{\phi}' &\equiv \frac{d\bar{\phi}}{d\eta} = v_\phi, \\ \bar{\phi}'' &\equiv \frac{dv_\phi}{d\eta},\end{aligned}\quad (66)$$

so that  $v_\phi$  is the conformal-time derivative of  $\bar{\phi}$ . Moreover, from Eq. (56) we have  $d\eta/dz = -1/H(z)$ , and hence  $\frac{dz}{d\eta} = -H(z)$ .

Since the redshift  $z$  is the primary observational variable (rather than the conformal time  $\eta$ ), it is useful to rewrite the background evolution equations in terms of  $z$ . We have already expressed the evolution equations for the Hubble parameter  $H$  and the scalar-field density parameter  $\Omega_\phi$  as functions of  $z$  in Eqs. (62) and (63). Using  $d\eta/dz = -1/H(z)$ , Eq. (65) can be recast as

$$\begin{aligned}\frac{dv_\phi}{dz} &= \frac{2(2-n)}{2n-1} \frac{v_\phi}{(1+z)} \\ &+ \frac{2^{n-1}}{n(2n-1)} \frac{v_\phi^{2-2n}}{H(z)(1+z)^{2n}} \left( \frac{dV}{d\bar{\phi}} \right),\end{aligned}\quad (67)$$

and the field itself obeys  $\frac{d\bar{\phi}}{dz} = \frac{d\bar{\phi}}{d\eta} \frac{d\eta}{dz} = -\frac{v_\phi}{H(z)}$ , where we used the definition in Eq. (66).

## V. METHODOLOGY AND DATA ANALYSIS WITH MODEL FITTING

In this section, we determine a set of present-day cosmological and field-theoretic quantities that characterize the background evolution: the Hubble constant  $H_0$ , the present matter density parameter  $\Omega_{m,0}$ , the scalar-field velocity  $v_{\phi,0}$ , the background field amplitude  $\bar{\phi}_0$ , and the kinetic (power-law) index  $n$ . These quantities are obtained by numerically integrating Eqs. (62)–(64) together with Eq. (67), subject to appropriate initial conditions. Among them,  $\bar{\phi}_0$ ,  $v_{\phi,0}$ , and  $n$  are model-specific parameters. The field amplitude  $\bar{\phi}_0$  sets the overall scale of the potential and therefore fixes the normalization of the scalar-field mass via  $m \propto \sqrt{V_0/\bar{\phi}_0}$ , where  $V_0 \equiv V(\bar{\phi}_0)$  denotes the present-day ( $z = 0$ ) value of the potential. For sufficiently small  $v_{\phi,0}$ , the kinetic contribution is subdominant to  $V(\bar{\phi}_0)$ , so the background scalar-field equation-of-state approaches  $\bar{w}_{\phi,0} \rightarrow -1$ , consistent with the  $\Lambda$ CDM limit. We work in natural units ( $c = \hbar = 1$ ), so all quantities are expressed in powers of energy. In this convention, a scalar field has mass (energy) dimension, hence  $\bar{\phi}_0$  is measured in energy units (typically eV) [46]. The velocity  $v_{\phi,0}$ , defined in Eq. (66) as a derivative with respect to conformal time  $\eta$  (which has dimension of inverse energy), therefore has units of energy squared, i.e. (eV)<sup>2</sup>. Finally,  $n$  is dimensionless.

We then confront the model predictions with a compilation of observational data, including Cosmic Chronometer (CC) measurements [101–111], Type Ia supernovae from the Pantheon+SHOES sample

[113, 134], Baryon Acoustic Oscillation (BAO) data [114–121], and the Gravitational-Wave Transient Catalogs (GWTC), namely GWTC-2.1 [9], GWTC-3 [10], and GWTC-4 [11, 122, 123]. Parameter constraints are obtained by minimizing the chi-squared statistic  $\chi^2(p)$ , which quantifies the residuals between theoretical predictions and observations weighted by the corresponding uncertainties. Assuming Gaussian errors, the likelihood is given by  $\mathcal{L}(p) \propto \exp[-\chi^2(p)/2]$ , so  $\chi^2$  minimization is equivalent to maximum-likelihood estimation and provides the basis for Bayesian posterior inference. Popular samplers such as *emcee*, *PyMC*, and *Stan* implement this (log-)likelihood when modeling data with Gaussian noise.

The expansion history of the universe, encoded in the Hubble parameter  $H(z)$ , is often inferred using distance-ladder techniques or standard candles such as Type Ia supernovae. An alternative and complementary approach is the Cosmic Chronometer (CC) method, first proposed in [101] and subsequently refined in [104]. In contrast to distance-based probes, the CC technique provides a direct and largely model-independent estimate of  $H(z)$  by exploiting the differential age evolution of passively evolving galaxies. In practice, one identifies *standard clocks*, typically massive early-type galaxies (ETGs), whose stellar populations evolve with minimal recent star formation.

Using the CC data listed in Table (II) (Appendix C), we quantify the goodness of fit through the usual chi-square statistic [115, 118]

$$\chi_{CC}^2 = \sum_{i=1}^{N=35} \left( \frac{H^{\text{th}}(z_i, \mathbf{p}) - H^{\text{obs}}(z_i)}{\sigma_{CC,i}} \right)^2, \quad (68)$$

where  $H^{\text{th}}(z_i, \mathbf{p})$  is the theoretical Hubble parameter obtained by solving Eq. (62) for a given parameter set  $\mathbf{p}$ ,  $H^{\text{obs}}(z_i)$  is the corresponding observational value, and  $\sigma_{CC,i}$  denotes the  $1\sigma$  uncertainty of the CC measurement reported in Table (II).

The *Pantheon+SHOES* compilation contains 1701 high-quality light-curve measurements corresponding to 1550 distinct Type Ia supernovae (SNe Ia), spanning the redshift range  $0.00122 \leq z \leq 2.2613$  [113, 134]. Cosmological constraints are obtained by statistically comparing the observed distance moduli inferred from the photometric data with the theoretical predictions of a given cosmological model. The distance modulus  $\mu(z, \theta)$  is defined as

$$\mu(z, \theta) = (m - M) = 5 \log_{10}(D_L(z)) + 25, \quad (69)$$

where  $m$  and  $M$  are the apparent and absolute magnitudes, respectively, and  $D_L(z)$  is the luminosity distance. For a spatially flat FLRW background it is given by [124]

$$D_L(z) = c(1+z) \int_0^z \frac{dz_1}{H(z_1)}, \quad (70)$$

with  $c$  the speed of light (in km/s) and  $H(z)$  in units of km/s/Mpc, so that  $D_L(z)$  is obtained in Mpc. Differentiating Eq. (70) with respect to  $z$  yields, we get the

equivalent differential equation of  $D_L(z)$  as mentioned in Eq. (61).

In our framework, Eq. (67) corresponds to the electromagnetic luminosity distance, i.e.  $D_L(z) \equiv D_L^{\text{EM}}(z)$ , consistent with the definitions introduced in Eqs. (60) and (61).

For the *Pantheon+SHOES* dataset, the full covariance matrix  $C$  (of dimension  $1701 \times 1701$ ) accounts for both statistical and systematic uncertainties in the set of observed distance moduli. The corresponding chi-square is therefore written as

$$\chi_{SN}^2 = \left( \mu_{\text{th}} - \mu_{\text{obs}} \right)^T C^{-1} \left( \mu_{\text{th}} - \mu_{\text{obs}} \right), \quad (71)$$

where  $\mu_{\text{th}} \equiv \mu_{\text{th}}(z_i, \mathbf{p})$  is computed from Eq. (66) (using the solutions of Eqs. (62), (63), and (68) for a given parameter set  $\mathbf{p}$ ),  $\mu_{\text{obs}} \equiv \mu_{\text{obs}}(z_i)$  denotes the observed moduli from Pantheon+SHOES [113, 134], and  $C^{-1}$  is the inverse covariance matrix.

Baryon acoustic oscillations (BAO) provide a robust standard ruler in observational cosmology and deliver stringent constraints on the expansion history of the Universe. Extracting the BAO feature from large-scale structure measurements (e.g., galaxy clustering) requires a set of cosmological distance measures to convert observed angular and redshift separations into comoving scales. In particular, the transverse comoving distance  $D_M(z)$ , the Hubble distance  $D_H(z)$ , and the volume-averaged distance  $D_V(z)$  play a central role. These quantities enable precise inference of key parameters, including the present-day Hubble constant  $H_0$  and the redshift-dependent dark-energy equation-of-state parameter  $w(z)$ , thereby providing critical tests of the  $\Lambda$ CDM model and its extensions such as  $w$ CDM.

In spectroscopic galaxy redshift surveys, the BAO signal is observed along both the radial (line-of-sight) and transverse (angular) directions, thereby encoding information about cosmic distances as well as the expansion rate of the universe. The radial component of the BAO feature, characterized by the redshift separation  $\Delta z$  associated with the sound-horizon scale, enables a direct estimate of the Hubble parameter via  $H(z) = c \Delta z / r_d$ . Here,  $r_d$  denotes the comoving sound horizon at the baryon drag epoch, i.e., the maximum distance that acoustic waves in the photon-baryon plasma could travel prior to baryon decoupling. It is given by [118, 119]

$$r_d = \int_{z_{\text{drag}}}^{\infty} \frac{c_s}{H(z)} dz \quad (72)$$

where  $z_{\text{drag}} (\approx 1020)$  denotes the baryon drag epoch, corresponding to the redshift at which baryons decouple from the photon-baryon fluid, and  $c_s$  is the sound speed within this plasma. In the present analysis,  $r_d$  is treated as a free parameter, allowing it to be directly constrained by observational data. The BAO feature also provides a measure of the Hubble distance at redshift  $z$ , defined as

$$D_H(z) = \frac{c}{H(z)}. \quad (73)$$

In the transverse direction, the BAO feature corresponds to a characteristic angular scale  $\Delta\theta = r_d / D_M(z)$ , i.e. the projection of the comoving sound horizon at redshift  $z$ . The transverse comoving distance  $D_M(z)$  depends on the expansion history and can be computed from Eq. (70) by replacing  $D_L(z)$  with  $D_M(z)$  [114–117].

When accounting for the cosmological dependence of  $r_d$ , BAO observations primarily constrain the dimensionless ratios  $D_M(z)/r_d$  and  $D_H(z)/r_d$ . Traditionally, BAO measurements were also reported using the spherically averaged (isotropic) distance  $D_V(z)$ , defined as [114–117]

$$D_V(z) = [z D_M(z)^2 D_H(z)]^{\frac{1}{3}}, \quad (74)$$

which combines radial and transverse information into a single observable. This compression is particularly useful at low redshift, where the sensitivity to anisotropies between line-of-sight and angular clustering is limited. In such cases,  $D_V(z)$  provides a convenient proxy for the geometric constraints from BAO, facilitating comparisons between cosmological models and parameter estimation.

In this work, we utilize two independent BAO datasets. The first, referred to as SDSSBAO, consists of 8 BAO measurements obtained from the *Sloan Digital Sky Survey (SDSS)* [114, 120]. The second dataset, denoted DESBAO, includes 9 BAO data points derived from the *Dark Energy Spectroscopic Instrument Data Release 2 (DESI DR2)* [121]. We combine these samples into a unified BAO dataset (17 data points in total). The datasets are listed in Tables III and IV (Appendix C). For the BAO likelihood [125, 126], we adopt a Gaussian chi-square of the form

$$\chi_{\text{BAO}}^2 = \sum_{i=1}^N \left( \frac{X^{\text{th}}(z_i, \mathbf{p}) - X^{\text{obs}}(z_i)}{\sigma_i} \right)^2, \quad (75)$$

where  $X^{\text{th}}(z_i, \mathbf{p})$  denotes the theoretical prediction for the BAO observable (e.g.,  $D_M(z_i)/r_d$ ,  $D_H(z_i)/r_d$ , or  $D_V(z_i)/r_d$ ), and  $X^{\text{obs}}(z_i)$  and  $\sigma_i$  are the corresponding measurements and uncertainties. When multiple BAO observables are included, the total BAO contribution is given by

$$\chi_{\text{BAO}}^2 = \chi_{D_M/r_d}^2 + \chi_{D_H/r_d}^2 + \chi_{D_V/r_d}^2. \quad (76)$$

We next describe the gravitational-wave (GW) datasets. GW astronomy provides an independent probe of the cosmic expansion history through standard sirens. Observations by the LIGO, Virgo, and KAGRA collaborations [127] have resulted in successive releases of the Gravitational-Wave Transient Catalogs (GWTC), which provide posterior distributions for source parameters—including the luminosity distance—that can be used for cosmological inference. In this work, we use luminosity-distance measurements from GWTC-2.1 [9], GWTC-3 [10], and GWTC-4 [11, 122, 123], which span multiple observing runs

and improve both the statistical power and redshift coverage of standard-siren analyses.

The GWTC-2.1 catalog [9] is an extended and refined version of GWTC-2 [8], based on a comprehensive reanalysis of events detected during the first half of the third observing run (O3a) of Advanced LIGO and Advanced Virgo. It includes confidently identified binary black-hole (BBH) mergers and previously reported sources such as binary neutron-star (BNS) systems. A key feature of GWTC-2.1 is its *deep* reanalysis, which employs improved data-quality vetting, mitigation of instrumental artifacts (glitches), and multiple matched-filter pipelines. By adopting a more permissive false-alarm-rate (FAR) threshold, the catalog reports additional high-confidence candidates and increases the number of significant O3a detections to 44. These methodological improvements yield more precise and reliable posterior distributions for source parameters, particularly the luminosity distance, which is central to standard-siren cosmology. Consequently, GWTC-2.1 provides a statistically rich dataset for intermediate-redshift standard-siren analyses.

The GWTC-3 catalog [10] provides a comprehensive compilation of detections from the full third observing run (O3), including both O3a and O3b. It substantially increases the sample of compact-binary coalescences, reporting 90 confident gravitational-wave events. The catalog includes a diverse population of sources, including binary black hole (BBH) mergers, binary neutron-star (BNS) mergers, and the first confirmed neutron-star-black-hole (NSBH) mergers (e.g., GW200105 and GW200115). The enlarged event sample strengthens population studies and enables more informative hierarchical analyses. Moreover, GWTC-3 extends the redshift reach of GW observations, improving constraints on the luminosity-distance-redshift relation. These advances are driven by improved detector sensitivity, refined waveform models, and (for a subset of events) the inclusion of KAGRA, which together enhance sky localization and help reduce degeneracies between luminosity distance and binary inclination. In a cosmological context, GWTC-3 provides an important foundation for *dark siren* analyses, in which GW luminosity distances are statistically associated with galaxy catalogs to infer cosmological parameters such as  $H_0$ .

The GWTC-4 catalog [11, 122, 123] reports detections from the first half of the fourth observing run (O4a), using data from Advanced LIGO, Advanced Virgo, and KAGRA operating at improved (“A+”) sensitivities. The rapid increase in the number of reported candidates substantially enlarges the event sample and enhances the statistical power of GW datasets. The inclusion of a multi-detector network improves sky localization and helps reduce degeneracies between luminosity distance and orbital inclination, enabling more precise parameter estimation. Increased sensitivity also extends the reach to higher-redshift compact-binary mergers, thereby probing the luminosity-distance-redshift relation in previously inaccessible regimes. In addition, the catalog includes several high-mass BBH events

that serve as useful laboratories for tests of gravity and cosmology. Owing to the larger number of high-confidence detections, statistical uncertainties on luminosity-distance measurements are reduced, making GWTC-4 particularly valuable for precision-cosmology applications. Overall, GWTC-4 provides a comprehensive dataset for constraining the expansion history of the universe, studying merger-rate evolution, and searching for potential deviations from standard cosmology, including modified GW propagation.

To incorporate the gravitational-wave (GW) luminosity-distance measurements from the GWTC-2.1 [9], GWTC-3 [10], and GWTC-4 [11, 122, 123] catalogs into our joint likelihood analysis, we construct a standard chi-square estimator for the GW sector [128]. The LVK collaboration [127] reports the GW luminosity distance  $D_L^{\text{GW}}(z)$  with asymmetric 90% credible intervals, quoted as upper and lower uncertainties  $\sigma_{\text{GW}}^+$  and  $\sigma_{\text{GW}}^-$ . These asymmetries reflect the non-Gaussian nature of the distance posterior and are driven mainly by the degeneracy between luminosity distance and binary inclination, together with detector noise properties. Following Refs. [128, 129], we approximate the asymmetric uncertainties by an effective symmetric standard deviation,

$$\sigma_{\text{GW}} = \frac{\sigma_{\text{GW}}^+ + \sigma_{\text{GW}}^-}{3.29}, \quad (77)$$

where the factor  $3.29 \simeq 2 \times 1.645$  converts a two-sided 90% credible interval to an equivalent Gaussian  $1\sigma$  uncertainty [9–11]. The GW contribution to the likelihood is then written as

$$\chi_{\text{GW}}^2 = \sum_{i=1}^N \left( \frac{D_L^{\text{GW,th}}(z_i, \mathbf{p}) - D_L^{\text{GW,obs}}(z_i)}{\sigma_{\text{GW},i}} \right)^2, \quad (78)$$

where  $D_L^{\text{GW,th}}(z_i, \mathbf{p})$  is the theoretical GW luminosity distance obtained by solving Eq. (61), and  $D_L^{\text{GW,obs}}(z_i)$  denotes the measured values from the GWTC catalogs. In our analysis, we consider three GW data combinations, namely GWTC (2.1+3), GWTC-4, and GWTC (2.1+3+4). For dimensional consistency, all reported  $D_L^{\text{GW}}$  values are converted from Gpc to Mpc.

We employed Bayesian inference using the No-U-Turn Sampler (NUTS) [130] to constrain the cosmological parameters  $\mathbf{p}$  from the OHD dataset. In this framework, Markov chain Monte Carlo (MCMC) sampling [131] is used to generate posterior distributions for the model parameters and to quantify the associated uncertainties. Point estimates are reported using the posterior mean values obtained from the MCMC chains. To assess the overall goodness of fit, we also compute the chi-square statistic, which measures the agreement between theoretical predictions and observational data. The resulting marginalized posteriors are visualized through 1D distributions and 2D contour plots, showing the  $1\sigma$  (68%) and  $2\sigma$  (95%) credible regions [132, 133] and highlighting parameter correlations in the multidimensional space.

## VI. RESULTS AND DISCUSSION

In our Bayesian inference framework, we adopt initial conditions and minimally informative uniform priors for the primary model parameters  $p = \{H_0, \Omega_{m,0}, v_{\phi,0}, \bar{\phi}_0, n, r_d\}$ , as listed in Table I. Here,  $\mathcal{U}(a, b)$  denotes a uniform prior over the interval  $(a, b)$ . These priors are chosen over physically motivated ranges to mitigate prior-driven biases while allowing the data to dominate the constraints. In particular, to guarantee a well-defined sound speed  $c_s^2$  with  $0 < c_s^2 \leq 1$  and to preserve causality in the interacting k-essence model, we restrict the kinetic index to  $n \sim \mathcal{U}(1.1, 1.9)$  (Table I). Figures 2 and 3 show the 1D marginalized posteriors and 2D contour plots, reporting the  $1\sigma$  and  $2\sigma$  credible intervals for the cosmological and model-specific parameters. Figure 2 presents the constraints from the joint CC+BAO+GWTC(2.1+3+4) analysis. As shown in Fig. 3, adding Pantheon+ data [134] substantially breaks residual background degeneracies, yielding our tightest and most robust constraints.

Measurements of the cosmic expansion rate from the cosmic microwave background (CMB), particularly those from the Planck Collaboration, favor a comparatively lower Hubble constant when interpreted within a flat  $\Lambda$ CDM cosmology. The 2018 analysis reports  $H_0 = 67.36 \pm 0.54 \text{ km s}^{-1} \text{ Mpc}^{-1}$  [90, 135]. This estimate was further consolidated in the subsequent legacy data release (public in 2020) [136], yielding a consistent value of  $H_0 \approx 67.4 \pm 0.5 \text{ km s}^{-1} \text{ Mpc}^{-1}$  and confirming the robustness of the CMB-based inference. In contrast, local (late-time) measurements, such as those from the SH0ES Collaboration [137], prefer a higher expansion rate,  $H_0 \approx 73.2 \pm 1.3 \text{ km s}^{-1} \text{ Mpc}^{-1}$ . The persistent discrepancy between these early- and late-universe determinations is commonly referred to as the ‘‘Hubble tension.’’

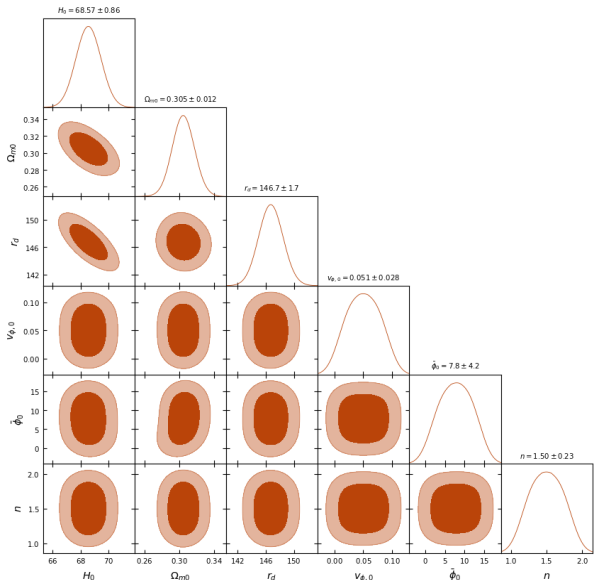


Figure 2: Fitting of model parameters with various combination of CC data, BAO data and GWTC (2.1 + 3 + 4) data.

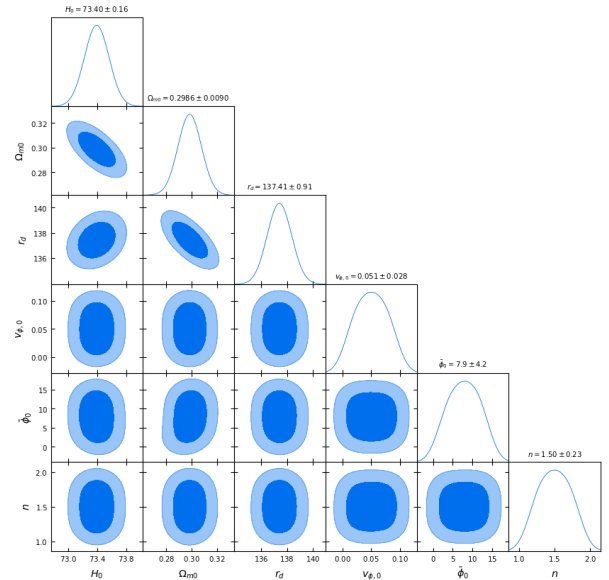


Figure 3: Fitting of model parameters with various combination of CC data, Pantheon data, BAO data and GWTC (2.1 + 3 + 4) data.

To constrain the cosmological parameters  $\{H_0, \Omega_{m,0}, r_d\}$  and the model-specific parameters  $\{v_{\phi,0}, \bar{\phi}_0, n\}$ , we perform Bayesian parameter inference using an MCMC approach. We find that combining complementary observational probes significantly improves the precision of the inferred parameters, yielding progressively tighter and more robust bounds. For the CC+BAO+GWTC combination (Fig. 2), we obtain  $H_0 = 68.57 \pm 0.86 \text{ km s}^{-1} \text{ Mpc}^{-1}$ , which is broadly consistent with expansion measurements. In contrast, the full joint analysis CC+Pantheon+BAO+GWTC (Fig. 3) yields our tightest constraint,  $H_0 = 73.40 \pm 0.16 \text{ km s}^{-1} \text{ Mpc}^{-1}$ , indicating a substantially higher late-time expansion rate. This result is in strong tension with the early-universe inference from Planck 2018 [136],  $H_0 = 67.4 \pm 0.5 \text{ km s}^{-1} \text{ Mpc}^{-1}$ , thereby reinforcing the persistence of the Hubble tension.

The same analyses also constrain the sound horizon at the drag epoch. From Fig. 2, we find  $r_d = 146.7 \pm 1.7 \text{ Mpc}$ , whereas the full dataset (Fig. 3) prefers a lower value,  $r_d = 137.41 \pm 0.91 \text{ Mpc}$ . The combination of a higher  $H_0$  and a reduced  $r_d$  reflects the well-known  $H_0$ – $r_d$  degeneracy, which acts as a compensatory mechanism to preserve agreement with distance measurements. This correlated shift is often interpreted as a potential signature of physics beyond standard  $\Lambda$ CDM and indicates that the k-essence framework has sufficient flexibility to alleviate the mismatch between early- and late-time inferences.

Using the joint CC + Pantheon + BAO + GWTC(2.1+3+4) dataset (Fig. 3 and Table I), which provides our best-fit constraints, we obtain  $\bar{\phi}_0 = 7.9 \pm 4.2 \text{ eV}$  for the present background scalar field,  $v_{\phi,0} = 0.051 \pm 0.028 (\text{eV})^2$  for the scalar-field velocity, and  $n = 1.50 \pm 0.23$  for the kinetic index. The inferred value  $n \simeq 1.5$  lies within the physically viable interval  $1 < n < 2$ , ensuring a well-defined sound

speed,  $0 < c_s^2 \leq 1$ . This points to a departure from canonical scalar-field dynamics and underscores the importance of the non-linear kinetic term in the Lagrangian  $\mathcal{L} = X^n - V(\phi)$ . The parameter  $v_{\phi,0}$  controls the present-day evolution of the field, enabling an effective cosmological-constant behavior while preserving dynamical freedom. Figures 7 and 8 (Appendix C) show the posterior correlation matrices for the parameter set  $p = \{H_0, \Omega_{m,0}, r_d, v_{\phi,0}, \bar{\phi}_0, n\}$  obtained from the CC + BAO + GWTC and the full CC + Pantheon + BAO + GWTC dataset, respectively.

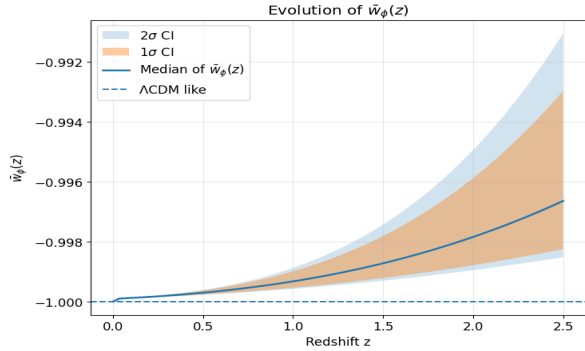


Figure 4: Plot of background scalar field EoS parameter  $\bar{w}_\phi(z)$  with redshift distance  $z$  with  $1\sigma$  and  $2\sigma$  credible interval (CI), using the best fitted parameters' values from our observational result.

Using these best-fit parameters, we reconstruct the evolution of the dark-energy sector. Figure 4 displays the redshift dependence of the background scalar-field equation-of-state (EoS) parameter,  $\bar{w}_\phi(z)$ . At the present epoch ( $z = 0$ ), we obtain the tight constraint  $\bar{w}_{\phi,0} = -0.9999999565 \pm 0.0000000777$ , showing that the k-essence field behaves essentially as a cosmological constant at late times. At higher redshifts, the widening credible bands and the small departures from  $w_{\text{de}} = -1$  (with  $w_{\text{de}}$  the dark-energy EoS) reflect the underlying dynamics induced by the non-canonical kinetic term. This feature is important, as it enables the model to interpolate between a more dynamical past and cosmological-constant-like behavior today.

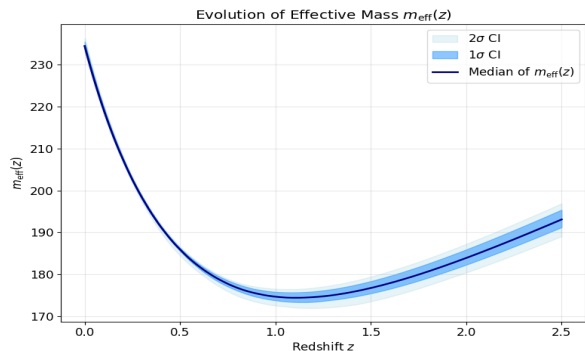


Figure 5: Evolution of the effective mass term  $m_{\text{eff}}$  as a function of redshift  $z$  with  $1\sigma$  and  $2\sigma$  credible interval (CI), using the best fitted parameters' values from our observational result.

A central result of our investigation is the evolution of the effective mass term  $m_{\text{eff}}(z)$  shown in Fig. 5. From the modified gravitational-wave equation (51),  $m_{\text{eff}}^2$  has the same mass dimension as  $k^2$ , so  $m_{\text{eff}}$  has units of inverse length (or inverse time) and therefore sets an energy scale in natural units ( $c = \hbar = 1$ ). Since the effective mass is sourced by cosmological background quantities via  $m_{\text{eff}}^2 \propto (\rho - P)$  in Eq. (49), a natural normalization is the Hubble scale in Eq. (59). In natural units,  $1 \text{ km s}^{-1} \text{ Mpc}^{-1} \simeq 10^{-42} \text{ GeV} \simeq 10^{-33} \text{ eV}$  [138], so our inferred values correspond to a physical scale  $m_{\text{eff}} \sim \mathcal{O}(10^{-33}) \text{ eV}$ , firmly in the ultra-light, cosmological regime.

For the best-fit dataset (CC + Pantheon + BAO + GWTC), the present-day value is tightly constrained to  $m_{\text{eff},0} \approx 234.51 \pm 1.04$ , which corresponds to an ultra-light physical scale of order  $10^{-33} \text{ eV}$  (using the unit conversion discussed above).

The parabolic evolution of  $m_{\text{eff}}$  in Fig. 5 reflects the transition from matter to dark-energy domination. At higher redshift, the larger matter density enhances  $m_{\text{eff}}$ , whereas at late times, as  $\bar{w}_{\phi,0} \rightarrow -1$ , the combination  $(\rho - P)$  approaches a constant and  $m_{\text{eff}}$  correspondingly stabilizes. In this sense,  $m_{\text{eff}}$  functions as a response of the cosmological medium, encoding how the joint matter and k-essence background modifies gravitational-wave propagation. Unlike scenarios that modify the wave speed, this mechanism preserves luminal propagation but induces a frequency-dependent phase shift, providing a characteristic observational signature of k-essence cosmology.

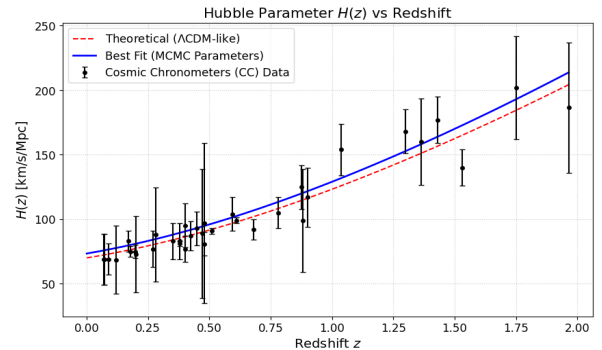


Figure 6: All available CC data points are in Table(II) (in Appendix C). Here the dashed red line plots the theoretical Hubble parameter  $H(z)$  as a function of redshift  $z$  with the typical values of  $\Omega_{\text{de},0} = 0.7$ ,  $\Omega_{m,0} = 0.3$  and  $H_0 = 70.0 \text{ km.s}^{-1}.\text{Mpc}^{-1}$  and the solid blue line plots  $H(z)$  as a function of redshift  $z$  with using the best fitted parameters' values from our observational result.

Finally, Fig. 6 compares the reconstructed Hubble parameter  $H(z)$  with cosmic chronometer measurements. The theoretical prediction (solid curve) is in good agreement with the data points over the full redshift range, indicating that the model reproduces the observed expansion history while simultaneously allowing for non-trivial and testable modifications in the gravitational-wave sector.

Table I: Cosmological model parameter constraints for different datasets. Here ‘GWTC’ means the combination of GWTC-2.1, GWTC-3 and GWTC-4 data.

Parameters	Prior	Datasets	
		CC + BAO + GWTC	CC + Pantheon + BAO + GWTC
$H_0$ [Km/s/Mpc]	$\mathcal{U}(60, 80)$	$68.57 \pm 0.86$	$73.40 \pm 0.16$
$\Omega_{m,0}$	$\mathcal{U}(0.2, 0.4)$	$0.305 \pm 0.012$	$0.2986 \pm 0.009$
$r_d$ [Mpc]	$\mathcal{U}(130, 160)$	$146.7 \pm 1.7$	$137.41 \pm 0.91$
$v_{\phi,0}$ [eV <sup>2</sup> ]	$\mathcal{U}(0.01, 0.1)$	$0.051 \pm 0.028$	$0.051 \pm 0.028$
$\bar{\phi}_0$ [eV]	$\mathcal{U}(0.1, 15.0)$	$7.8 \pm 4.2$	$7.9 \pm 4.2$
$n$	$\mathcal{U}(1.1, 1.9)$	$1.5 \pm 0.23$	$1.50 \pm 0.23$

An interesting aspect of the present framework concerns the possible implications of the redshift evolution of the effective tensor mass  $m_{\text{eff}}(z)$  for the inferred Hubble constant  $H_0$ . Because  $m_{\text{eff}}$  is fixed by the background dynamics of the k-essence sector, the same non-canonical physics that generates dispersive GW propagation can also modify the late-time expansion history and, consequently, shift the cosmological parameters inferred from data. In this sense, the model provides an alternative phenomenological mechanism for producing small deviations from standard  $\Lambda$ CDM while remaining compatible with current gravitational-wave constraints.

Accordingly, the non-canonical k-essence dynamics may alter the late-time behavior of  $H(z)$  and the effective dark-energy equation of state, which can impact distance indicators and the inferred value of  $H_0$ . While the present analysis is not intended to provide a complete resolution of the Hubble tension, our results suggest that the evolution of  $m_{\text{eff}}(z)$  and the underlying scalar-field dynamics can contribute to alleviating the discrepancy between early- and late-time determinations.

Finally, the model preserves the luminal GW speed,  $c_{\text{gw}} = 1$ , while still allowing dispersive phase corrections through  $m_{\text{eff}}$ , making it phenomenologically attractive: unlike many modified-gravity scenarios constrained by multimessenger observations, the present framework remains compatible with GW170817 while permitting nontrivial late-time cosmological effects.

Overall, this combined analysis shows that the k-essence framework provides a viable fit to current cosmological datasets and offers a consistent mechanism that can alleviate the Hubble tension, while predicting distinctive signatures in gravitational-wave propagation. A more detailed statistical analysis—including a full Bayesian comparison with the standard  $\Lambda$ CDM model, together with a combined analysis of CMB, gravitational-wave, and other data—would be necessary to quantify the precise impact of the model on the  $H_0$  tension. Such a comprehensive observational analysis, in which early-universe CMB data are used to set boundary conditions and the study is restricted to  $z \geq 1.9$ , is beyond the scope of the present work and will be addressed in future investigations.

## VII. CONCLUSION

In this work, we have presented a combined theoretical and observational study of the propagation of linearized gravitational waves (GWs) in k-essence cosmology, in which the dark sector is described by a non-canonical scalar field. Starting from tensor perturbations on a curved FLRW background and adopting the high-frequency (short-wavelength) limit, we derived a modified gravitational-wave evolution equation that encodes the impact of the background scalar-field dynamics. Within the same homogeneous and isotropic setting, and under the weak-field approximation, we showed that this tensor-mode evolution consistently captures the influence of the non-canonical k-essence sector on GW propagation. A central outcome is the appearance of a time-dependent effective mass-like term,  $m_{\text{eff}}$ , for tensor modes, sourced by both cosmological expansion and the non-canonical structure of the k-essence Lagrangian.

Importantly, the model preserves luminal gravitational-wave propagation ( $c_{\text{gw}} = 1$ ), in agreement with stringent multimessenger bounds (e.g., GW170817), while still yielding a non-trivial modification of the dispersion relation. Specifically, the k-essence background induces an ultra-light effective mass term  $m_{\text{eff}}$  for tensor modes. This contribution leaves the number of propagating degrees of freedom unchanged, but generates a cumulative, frequency-dependent phase shift  $\Delta\Theta$  in GW signals that builds up over cosmological distances. The resulting dispersive imprint provides a potential observational handle on the microphysics of dark energy. Moreover, we found that  $m_{\text{eff}}$  depends explicitly on cosmological background quantities, including the Hubble parameter and the scalar-field equation-of-state parameter  $\bar{w}_\phi$ , thereby linking GW observables directly to the underlying expansion history and k-essence dynamics.

We further considered a specific class of k-essence models with a power-law kinetic term and a quadratic potential (44). In this setting, we recast the modified gravitational-wave equation in redshift space, which facilitates a direct comparison with data. We then performed a joint Bayesian inference using Cosmic Chronometers, BAO, Pantheon+ supernovae, and GW standard-siren information from the GWTC-2.1,

GWTC-3, and GWTC-4 catalogs. We find that the model is consistent with current constraints and reproduces the observed late-time expansion history. The data tightly constrain the present-day effective mass to  $m_{\text{eff},0} \equiv m_{\text{eff}}(z=0) \approx 234.51 \pm 1.04$ , corresponding to an ultra-light physical scale of  $\mathcal{O}(10^{-33})$  eV. Notably, the background-induced mass provides a physically motivated mechanism that may help alleviate the Hubble tension, without requiring deviations in the gravitational-wave speed or additional amplitude damping. Overall, our results indicate that this k-essence scenario is compatible with contemporary cosmological datasets while offering a plausible pathway to address existing cosmological tensions.

Overall, this study highlights gravitational waves as precision probes of the cosmological background and identifies dispersive propagation as a robust, testable signature of non-canonical scalar-field (k-essence) models. The framework developed here constitutes a consistent and observationally viable extension of standard cosmology, in which departures from general relativity appear primarily as phase-level corrections rather than as kinematic anomalies. Ultimately, our results show that fine-grained dispersive imprints in gravitational-wave signals can probe the microphysics of dark energy without requiring any deviation from the fundamental speed of light.

Several directions could extend and deepen this analysis. First, moving beyond linear perturbation theory to second order would enable a systematic study of scalar-tensor couplings. Second, exploring more general k-essence models, or embedding the framework within Horndeski and beyond-Horndeski (DHOST) theories, could uncover richer phenomenology, including modifications to gravitational-wave amplitude and polarization, as well as the redshift evolution of the effective mass term driven by non-minimal couplings.

Third, a waveform-level analysis within full parameter-estimation pipelines for current ground-based detectors (LIGO, Virgo, and KAGRA), as well as future observatories (LISA, Taiji, TianQin, the Einstein Telescope, and Cosmic Explorer), will be essential to quantify the detectability of the predicted cumulative phase shifts and to constrain key parameters such as the kinetic index  $n$  and the scalar-field potential  $V(\phi)$ . Finally, combining gravitational-wave

measurements with large-scale-structure probes and cosmic microwave background (CMB) data could help break parameter degeneracies. Extending the framework to early-universe scenarios—including inflationary tensor modes and stochastic gravitational-wave backgrounds—may provide further insight into the origin and evolution of the dark sector. These directions are left for future work and are beyond the scope of the present analysis.

## ACKNOWLEDGMENTS

G.M. (IUCAA Associate) acknowledges the Inter-University Centre for Astronomy and Astrophysics (IUCAA), Pune, India, for facilitating part of this work during his visit. G.M. and E.G. thank the COST Association (CA21136 CosmoVerse), European Union, for the opportunity to participate in this international association as group members. E.G. also thanks the COST Association (CA23130, BridgeQG), European Union, for the opportunity to participate in this international association as a group member. G.M. extends his gratitude to all undergraduate, postgraduate, and doctoral students, along with his teachers, collaborators, and well-wishers, whose support has significantly enriched his academic journey. S.B. gratefully acknowledges his parents for their constant love, encouragement, and unwavering support throughout every stage of his academic and personal journey.

**Conflicts of interest:** The authors declare no conflicts of interest.

**Funding information:** Not available.

**Data availability:** The data used in this study are readily accessible from public sources for validation of our model; however, we did not generate any new data sets for this research.

- 
- [1] A. Einstein, “Naherungsweise Integration der Feldgleichungen der Gravitation”, *Sitzungsberichte der Koniglich Preussischen Akademie der Wissenschaften (Berlin)*, 688–696, (1916), <https://doi.org/10.34663/9783945561317-04>
- [2] H. Bondi, M. G. J. Van der Burg and M. G. J. Van der Burg, “Gravitational waves in general relativity, VII. Waves from axi-symmetric isolated system Available to Purchase”, *Proc.Roy.Soc.Lond.A* **269**, 21-52, (1962), <https://doi.org/10.1098/rspa.1962.0161>
- [3] R. K. Sachs, “Gravitational waves in general relativity. VIII. Waves in asymptotically flat space-time.”, *Proc. Roy. Soc. London Ser. A* **270**, 103–126, (1962), <https://doi.org/10.1098/rspa.1962.0206>
- [4] J. H. Taylor and J. M. Weisberg, “A new test of general relativity - Gravitational radiation and the binary pulsar PSR 1913+16”, *Astrophys. Jour.*, **253**, p. 908-920. (1982), <https://doi.org/10.1086/159690>
- [5] R. A. Hulse and J. H. Taylor, “Discovery of a pulsar in a binary system”, *Astrophys. Jour.*, **195**, p. L51-L53, (1975), <https://doi.org/10.1086/181708>
- [6] B.P. Abbott, et al. (LIGO Scientific Collaboration and Virgo Collaboration) “Observation of Gravitational Waves from a Binary Black Hole Merger”, *Phys. Rev. Lett.* **116**, 061102, (2016), <https://doi.org/10.1103/PhysRevLett.116.061102>

- [7] B. P. Abbott, et al. (LIGO Scientific Collaboration and Virgo Collaboration), “GWTC-1: A Gravitational-Wave Transient Catalog of Compact Binary Mergers Observed by LIGO and Virgo during the First and Second Observing Runs”, *Phys. Rev. X* **9**, 031040, (2019), <https://doi.org/10.1103/PhysRevX.9.031040>
- [8] R. Abbott, et al. (The LIGO Scientific Collaboration and the Virgo Collaboration), “GWTC-2: Compact Binary Coalescences Observed by LIGO and Virgo during the First Half of the Third Observing Run”, *Phys. Rev. X* **11**, 021053, (2021), <https://doi.org/10.1103/PhysRevX.11.021053>
- [9] R. Abbott, et al. (The LIGO Scientific Collaboration and the Virgo Collaboration), “GWTC-2.1: Deep extended catalog of compact binary coalescences observed by LIGO and Virgo during the first half of the third observing run”, *Phys. Rev. D* **109**, 022001, (2024), <https://doi.org/10.1103/PhysRevD.109.022001>
- [10] R. Abbott, et al. (The LIGO Scientific Collaboration and the Virgo Collaboration), “GWTC-3: Compact Binary Coalescences Observed by LIGO and Virgo during the Second Part of the Third Observing Run”, *Phys. Rev. X* **13**, 041039, (2023), <https://doi.org/10.1103/PhysRevX.13.041039>
- [11] A. G. Abac, et al. (The LIGO Scientific Collaboration, the Virgo Collaboration, the KAGRA Collaboration), “GWTC-4.0: Updating the Gravitational-Wave Transient Catalog with Observations from the First Part of the Fourth LIGO-Virgo-KAGRA Observing Run”, arXiv:2508.18082, (2025), <https://doi.org/10.48550/arXiv.2508.18082>
- [12] B. Schutz, “Determining the Hubble constant from gravitational wave observations”, *Nature* **323**, (1986), <https://doi.org/10.1038/323310a0>
- [13] D. E. Holz and S. A. Hughes, “Using Gravitational-Wave Standard Sirens”, *Astrophys. Jour.* **629**, 15, (2005), <https://doi.org/10.1086/431341>
- [14] M. Maggiore, *Gravitational Waves: Theory and Experiments (Vol. 1)*, Oxford Univ. Press, Oxford, (2008).
- [15] É. É Flanagan, S. A Hughes, “The basics of gravitational wave theory”, *New J. Phys.* **7** (2005) 204, <http://doi.org/10.1088/1367-2630/7/1/204>
- [16] B. P. Abbott et al. (LIGO Scientific Collaboration and Virgo Collaboration), “GW170817: Observation of Gravitational Waves from a Binary Neutron Star Inspiral”, *Phys. Rev. Lett.* **119**, 161101, (2017) <https://doi.org/10.1103/PhysRevLett.119.161101>
- [17] B. P. Abbott et al. “Gravitational Waves and Gamma-Rays from a Binary Neutron Star Merger: GW170817 and GRB 170817A”, *Astrophys. Jour.*, **848**, L13, (2017), <https://doi.org/10.3847/2041-8213/aa920c>
- [18] E. Belgacem, et. al., “Testing modified gravity at cosmological distances with LISA standard sirens”, *JCAP*, **07**, 024, (2019), <https://doi.org/10.1088/1475-7516/2019/07/024>
- [19] A. Nishizawa, “Generalized framework for testing gravity with gravitational-wave propagation. I. Formulation”, *Phys. Rev. D* **97**, 104037, (2018), <https://doi.org/10.1103/PhysRevD.97.104037>
- [20] G. W. Horndeski, “Second-order scalar-tensor field equations in a four-dimensional space”, *Int. J. Theor. Phys.* **10**, 363–384, (1974), <https://doi.org/10.1007/BF01807638>
- [21] C. Deffayet, X. Gao, D. A. Steer, and G. Zahariade, “From  $k$ -essence to generalized Galileons”, *Phys. Rev. D* **84**, 064039, (2011), <https://doi.org/10.1103/PhysRevD.84.064039>
- [22] T. Kobayashi, M. Yamaguchi and J. Yokoyama, “Generalized G-inflation: Inflation with the most general second-order field equations”, *Prog. Theor. Phys.* **126**, 511-529, (2011), <https://doi.org/10.1143/PTP.126.511>
- [23] L. Lombriser and A. Taylor, “Breaking a Dark Degeneracy with Gravitational Waves”, *JCAP* **03**, 031, (2016), <https://doi.org/10.1088/1475-7516/2016/03/031>
- [24] P. Creminelli and F. Vernizzi, “Dark Energy after GW170817 and GRB170817A”, *Phys. Rev. Lett.* **119**, 251302, (2017), <https://doi.org/10.1103/PhysRevLett.119.251302>
- [25] J. M. Ezquiaga, and M. Zumalacárregui, “Dark Energy After GW170817: Dead Ends and the Road Ahead”, *Phys. Rev. Lett.* **119**, 251304, (2017), <https://doi.org/10.1103/PhysRevLett.119.251304>
- [26] T. Baker, E. Bellini, P. G. Ferreira, M. Lagos, J. Noller, and I. Sawicki, “Strong Constraints on Cosmological Gravity from GW170817 and GRB 170817A”, *Phys. Rev. Lett.* **119**, 251301, (2017), <https://doi.org/10.1103/PhysRevLett.119.251301>
- [27] C. Armendariz-Picon, V. F. Mukhanov and P. J. Steinhardt, “Dynamical Solution to the Problem of a Small Cosmological Constant and Late-Time Cosmic Acceleration”, *Phys. Rev. Lett.* **85**, 4438, (2000), <https://doi.org/10.1103/PhysRevLett.85.4438>
- [28] C. Armendariz-Picon, V. F. Mukhanov, P. J. Steinhardt, “Essentials of  $k$ -essence”, *Phys. Rev. D* **63**, 103510, (2001), <https://doi.org/10.1103/PhysRevD.63.103510>
- [29] J Garriga, V. F. Mukhanov, “Perturbation in  $k$ -inflation”, *Phys. Lett. B* **438** (2-3) (1999) 219-225, [https://doi.org/10.1016/S0370-2693\(99\)00602-4](https://doi.org/10.1016/S0370-2693(99)00602-4).
- [30] C. M. Will, “Bounding the mass of the graviton using gravitational-wave observations of inspiralling compact binaries”, *Phys. Rev. D* **57**, 2061, (1998), <https://doi.org/10.1103/PhysRevD.57.2061>
- [31] S. Mirshekari, N. Yunes, and C. M. Will, “Constraining Lorentz-violating, modified dispersion relations with gravitational waves”, *Phys. Rev. D* **85**, 024041, (2012), <https://doi.org/10.1103/PhysRevD.85.024041>
- [32] R. A. Isaacson, “Gravitational Radiation in the Limit of High Frequency. I. The Linear Approximation and Geometrical Optics”, *Phys. Rev.* **166**, 1263, (1968), <https://doi.org/10.1103/PhysRev.166.1263>
- [33] R. A. Isaacson, “Gravitational Radiation in the Limit of High Frequency. II. Nonlinear Terms and the Effective Stress Tensor”, *Phys. Rev.* **166**, 1272, (1968), <https://doi.org/10.1103/PhysRev.166.1272>
- [34] M. Maggiore, *Gravitational Waves: Astrophysics and Cosmology (Vol. 2)*, Oxford Univ. Press, Oxford, (2018).
- [35] R. M. Wald, *General Relativity*, The University of Chicago Press, (1984).
- [36] S. M. Carroll, *Spacetime and Geometry: An Introduction to General Relativity*, Cambridge University Press, (2019)
- [37] B. Schutz, *A First Course in General Relativity*, Cambridge University Press, (2012), <https://doi.org/10.1017/CB09780511984181>
- [38] M. Blau, *Lecture Notes on General Relativity*, Albert Einstein Center for Fundamental Physics, Bern Uni-

- versity, (2022), <http://www.blau.itp.unibe.ch/GRlecturenotes.html>
- [39] S. Mondal, et al., “Propagation of gravitational waves in various cosmological backgrounds”, *Gen. Rel. Grav.* **53** (7) (2021) 64, <https://doi.org/10.1007/s10714-021-02835-x>
- [40] C. Armendariz-Picon, T. Damour, V. Mukhanov, “ $k$ -inflation”, *Phys. Lett. B* **458**, 209-218, (1999), [https://doi.org/10.1016/S0370-2693\(99\)00603-6](https://doi.org/10.1016/S0370-2693(99)00603-6)
- [41] A. Vikman, “K-essence: Cosmology, causality and Emergent Geometry”, Dissertation an der Fakultät für Physik, Arnold Sommerfeld Center for Theoretical Physics, der LudwigMaximilians-Universität München, München (2007).
- [42] M. Malquarti, E. J. Copeland, A. R. Liddle, M. Trodden, “A new view of  $k$ -essence”, *Phys. Rev. D* **67**, 123503, (2003), <https://doi.org/10.1103/PhysRevD.67.123503>
- [43] L. P. Chimento, A. Feinstein, “Power - law expansion in  $k$ -essence cosmology”, *Mod.Phys.Lett.A* **19**, 761-768, (2004), <https://doi.org/10.1142/S0217732304013507>
- [44] P. Jorge, J. P. Mimoso, D. Wands, “On the dynamics of  $k$ -essence models”, *J. Phys.: Conf. Ser.* **66**, 012031, (2007), <https://doi.org/10.1088/1742-6596/66/1/012031>
- [45] S. Ganguly et. al., “Non-Affine Extensions of the Raychaudhuri Equation in the K-essence Framework”, *Phys. Lett. B*, **868**, 139622, (2025) <https://doi.org/10.1016/j.physletb.2025.139622>
- [46] S. Ganguly et al., “Observational Insights on DBI K-essence Models Using Machine Learning and Bayesian Analysis,” *Forts. der Phys.*, **74**, e70117, (2026) <https://doi.org/10.1002/prop.70117>
- [47] K. Bamba, J. Matsumoto, S. Nojiri, “Cosmological perturbations in k-essence model,” *Phys. Rev. D* **85**, 084026, (2012), <https://doi.org/10.1103/PhysRevD.85.084026>
- [48] T. Padmanabhan and T. Roy Choudhury, “Can the clustered dark matter and the smooth dark energy arise from the same scalar field?”, *Phys. Rev. D* **66**, 081301, (2002), <https://doi.org/10.1103/PhysRevD.66.081301>
- [49] T. Chiba, ‘Tracking k-Essence’. *Phys. Rev. D*, **66**, 6, 063514, (2002). <https://doi.org/10.1103/PhysRevD.66.063514>
- [50] S. Das, A. Panda, G. Manna, S. Ray, ‘Raychaudhuri Equation in K -essence Geometry: Conditional Singular and Non-Singular Cosmological Models’, *Fortschr. Phys.*, **71**, 4-5, 2200193, (2023). <https://doi.org/10.1002/prop.202200193>
- [51] G. Manna, “Gravitational collapse for the K-essence emergent Vaidya spacetime”, *Eur. Phys. J. C*, **80**, 9, 813, (2020). <https://doi.org/10.1140/epjc/s10052-020-8383-y>.
- [52] G. Manna, P. Majumdar, and B. Majumder, “K-essence emergent spacetime as a generalized Vaidya geometry”, *Phys. Rev. D*, **101**, 12, 124034, (2020). <https://doi.org/10.1103/PhysRevD.101.124034>.
- [53] A. Panda, D. Gangopadhyay, G. Manna “Form Invariance of Raychaudhuri equation in the presence of Inflaton-type fields.”, *Fortschr. Phys.*, **72**, 9–10, 2400134, (2024). [doi:10.1002/prop.202400134](https://doi.org/10.1002/prop.202400134).
- [54] S. Dodelson, F. Schmidt, *Modern Cosmology*, Second Edition, Academic Press, (2020)
- [55] K. Roy, D. Gangopadhyay, C. Singha, G. Manna, “Boltzmann Dynamics in K-essence Cosmology: Photon Propagation in an Emergent Spacetime”, <https://doi.org/10.48550/arXiv.2602.19576>
- [56] C. Cheung, P. Creminelli, A. L. Fitzpatrick, J. Kaplan, and L. Senatore, “The effective field theory of inflation,” *JHEP* **03**, 014 (2008), <https://doi.org/10.1088/1126-6708/2008/03/014>
- [57] J. Gleyzes, D. Langlois, F. Piazza, and F. Vernizzi, “New Class of Consistent Scalar-Tensor Theories,” *Phys. Rev. Lett.* **114**, 211101 (2015), <https://doi.org/10.1103/PhysRevLett.114.211101>
- [58] M. Zumalacarregui and J. Garcia-Bellido, “Transforming gravity: From derivative couplings to matter to second-order scalar-tensor theories beyond the Horndeski Lagrangian,” *Phys. Rev. D* **89**, 064046 (2014), <https://doi.org/10.1103/PhysRevD.89.064046>
- [59] B. Das, N. Jaman and M. Sami, “Gravitational wave background from quintessential inflation and NANOGrav data”, *Phys. Rev. D* **108**, 103510, (2023), <https://doi.org/10.1103/PhysRevD.108.103510>
- [60] K. Kohri, T. Terada, “Semianalytic calculation of gravitational wave spectrum nonlinear induced from primordial curvature perturbations”, *Phys. Rev. D* **97**, 123532 (2018), <https://doi.org/10.1103/PhysRevD.97.123532>.
- [61] J. Li, G. H. Guo, “Measuring the scalar induced gravitational waves from observation”, *Eur. Phys. J. C* (2021) 81:602, <https://doi.org/10.1140/epjc/s10052-021-09405-0>.
- [62] K. N. Ananda, C. Clarkson and D. Wands, “Cosmological gravitational wave background from primordial density perturbations”, *Phys. Rev. D* **75**, 123518 (2007), <https://doi.org/10.1103/PhysRevD.75.123518>
- [63] O. Sergijenko, B. Novosyadly, “Sound speed of scalar field dark energy: Weak effects and large uncertainties”, *Phys. Rev. D* **91**, 083007, (2015), <https://doi.org/10.1103/PhysRevD.91.083007>
- [64] M. Kunz, , S. Nesseris, I. Sawicki, “Using dark energy to suppress power at small scales”, *Phys. Rev. D* **92**, 063006, (2015), <https://doi.org/10.1103/PhysRevD.92.063006>
- [65] M. Bouhmadi-López, K. S. Kumar, J. Marto, J. Morais, A. Zhuk, “K-essence model from the mechanical approach point of view: coupled scalar field and the late cosmic acceleration”, *JCAP* **07**, 050, (2016), <https://doi.org/10.1088/1475-7516/2016/07/050>
- [66] B. R. Dinda, N. Banerjee, “Constraints on the speed of sound in the  $k$ -essence model of dark energy”, *Eur. Phys. J. C* **84** :177, (2024), <https://doi.org/10.1140/epjc/s10052-024-12547-6>
- [67] A. De Felice, S. Tsujikawa, “Inflationary non-Gaussianities in the most general second-order scalar-tensor theories”, *Phys. Rev. D* **84**, 083504, (2011), <https://doi.org/10.1103/PhysRevD.84.083504>
- [68] T. Kobayashi, “Horndeski theory and beyond: a review”, *Rept. Prog. Phys.* **82**, 086901, (2019), <https://doi.org/10.1088/1361-6633/ab2429>
- [69] A. Chakraborty, A. Ghosh and N. Banerjee, “Dynamical systems analysis of a k-essence model,” *Phys. Rev. D* **99**, no.10, 103513, (2019) <https://doi.org/10.1103/PhysRevD.99.103513>
- [70] R. Herrera and C. Rios, “Reconstructing inflation in a generalized Rastall theory of gravity,” *Nucl. Phys. B* **1022**, 117246, (2026), <https://doi.org/10.1016/j.nuclphysb.2025.117246>
- [71] H. Assadullahi and D. Wands, “Gravitational

- waves from an early matter era”, *Phys. Rev. D* **79**, 083511, (2009), <https://doi.org/10.1103/PhysRevD.79.083511>
- [72] C. Cheung, P. Creminelli, A. L. Fitzpatrick, J. Kaplan, and L. Senatore, “The effective field theory of inflation,” *JHEP* **03**, 014 (2008), <https://doi.org/10.1088/1126-6708/2008/03/014>
- [73] G. Gubitosi, F. Piazza, and F. Vernizzi, “The effective field theory of dark energy,” *JCAP* **02**, 032 (2013), <https://doi.org/10.1088/1475-7516/2013/02/032>
- [74] D. Baumann, P. Steinhardt, and K. Takahashi, “Gravitational wave spectrum induced by primordial scalar perturbations,” *Phys. Rev. D* **76**, 084019, (2007) <http://dx.doi.org/10.1103/PhysRevD.76.084019>
- [75] J. K. Bloomfield, È. È. Flanagan, M. Park, and S. Watson, “Dark energy or modified gravity? An effective field theory approach,” *JCAP* **08**, 010 (2013), <https://doi.org/10.1088/1475-7516/2013/08/010>
- [76] E. Bellini and I. Sawicki, “Maximal freedom at minimum cost: linear large-scale structure in general modifications of gravity,” *JCAP* **07**, 050 (2014), <https://doi.org/10.1088/1475-7516/2014/07/050>
- [77] J. Sakstein and B. Jain, “Implications of the Neutron Star Merger GW170817 for Cosmological Scalar-Tensor Theories”, *Phys. Rev. Lett.* **119**, 251303, (2017), <https://doi.org/10.1103/PhysRevLett.119.251303>
- [78] E. Belgacem, Y. Dirian, S. Foffa, and M. Maggiore, “Gravitational-wave luminosity distance in modified gravity theories”, *Phys. Rev. D* **97**, 104066, (2018), <https://doi.org/10.1103/PhysRevD.97.104066>
- [79] P. Jones, P. Pradhan and D. Singleton, “Signatures of Electromagnetic and Sound Radiation Produced by Gravitational Waves in Core-collapse Supernovae”. *Astrophys. Jour.* **989**, 18, (2025), <https://doi.org/10.3847/1538-4357/adea3e>
- [80] P. Jones, et al., “Gravitational-wave optics and intensity correlations for binary inspiral signal detections”. *Int. J. Mod. Phys. D.* **38**, 2330005 (2023), <https://doi.org/10.1142/S0217751X23300053>
- [81] A. Barrett and P. Jones, “Second Order Glauber Correlation of Gravitational Waves Using the LIGO Observatories as Hanbury Brown and Twiss Detectors”, *Phys. Sci. Forum* **25**, (2021), <https://doi.org/10.3390/ECU2021-09519>
- [82] P. Jones and D. Singleton, “Interaction between gravitational radiation and electromagnetic radiation”. *Int. J. Mod. Phys. D.*, **28**, 1930010, (2019), <https://doi.org/10.1142/S0218271819300106>
- [83] A. Gretarsson, P. Jones, and D. Singleton, “Gravity’s light in the shadow of the Moon”. *Int. J. Mod. Phys. D.*, **27**, 1847021 (2018), <https://doi.org/10.1142/S0218271818470211>
- [84] P. Jones and D. Singleton, “Gravitons to photons — Attenuation of gravitational waves”. *Int. J. Mod. Phys. D.*, **24**, 1544017, (2015), <https://doi.org/10.1142/S0218271815440174>
- [85] P. Jones, P. McDougall and D. Singleton, “Particle production in a gravitational wave background”, *Phys. Rev. D* **95**, 065010, (2017), <https://doi.org/10.1103/PhysRevD.95.065010>
- [86] P. Jones, P. McDougall, M. Ragsdale and D. Singleton, “Scalar field vacuum expectation value induced by gravitational wave background”, *Phys. Lett. B.* **781**, (2018), <https://doi.org/10.1016/j.physletb.2018.04.055>
- [87] L. D. Landau and E. M. Lifshitz, “The Classical Theory of Fields: Volume 2”, Butterworth-Heinemann, (1975), [https://books.google.com/books/about/The\\_Classical\\_Theory\\_of\\_Fields.html?id=X18PF4oKyrUC](https://books.google.com/books/about/The_Classical_Theory_of_Fields.html?id=X18PF4oKyrUC).
- [88] J.T Mendonca, “Theory of Photon Acceleration”, CRC Press, (2000), <https://doi.org/10.1201/9780367801472>.
- [89] F. F. Chen. “Introduction to Plasma Physics and Controlled Fusion”, Springer, (2015), <https://doi.org/10.1007/978-3-319-22309-4>
- [90] N. Aghanim, et al., Planck Collaboration, “Planck 2018 results. VI. Cosmological parameters”, *Astron. Astrophys.* **641** (2020) A6, <http://dx.doi.org/10.1051/0004-6361/201833910>.
- [91] M. Chevallier and D. Polarski, “Accelerating universes with scaling dark matter,” *Int. J. Mod. Phys. D* **10** (2001) 213–224, <https://doi.org/10.1142/S0218271801000822>.
- [92] E. V. Linder, “Exploring the expansion history of the universe,” *Phys. Rev. Lett.* **90** (2003) 091301, <https://doi.org/10.1103/PhysRevLett.90.091301>.
- [93] N. Bose and A. S. Majumdar, “*k*-essence model of inflation, dark matter, and dark energy.”, *Phys. Rev. D* **79**, 103517, (2009), <https://doi.org/10.1103/PhysRevD.79.103517>
- [94] J. De-Santiago and J. L. Cervantes-Cota, “Generalizing a unified model of dark matter, dark energy, and inflation with a noncanonical kinetic term”, *Phys. Rev. D* **83**, 063502, (2011), <https://doi.org/10.1103/PhysRevD.83.063502>
- [95] W. Fang, H Q Lu and Z G Huang, “Cosmologies with a general non-canonical scalar field”, *Class. Quantum Grav.* **24**, 3799, (2007), <https://doi.org/10.1088/0264-9381/24/15/002>
- [96] V. F. Mukhanov and A. Vikman, “Enhancing the tensor-to-scalar ratio in simple inflation”, *JCAP* **02**, 004, (2006), <https://doi.org/10.1088/1475-7516/2006/02/004>
- [97] V. Mukhanov and H. A. Feldman and R. H. Brandenberger, “Theory of Cosmological Perturbations”, *Phys. Rept.*, **215**, 203–333, (1992)
- [98] V. Mukhanov, “Physical Foundation of Cosmology”, Cambridge University Pres, Cambridge, (2005)
- [99] N. D. Birrell and P. C. W. Davies, “Quantum Fields in Curved Space,” Cambridge University Pres, Cambridge, (1984)
- [100] S. Unnikrishnan, V. Sahni and A. Toporensky, “Refining inflation using non-canonical scalars”, *JCAP* **08**, 018, (2012), <https://doi.org/10.1088/1475-7516/2012/08/018>
- [101] R. Jimenez and A. Loeb, “Constraining Cosmological Parameters Based on Relative Galaxy Ages”, *Astrophys. Jour.*, **573**, 37, (2002), <http://dx.doi.org/10.1086/340549>
- [102] C. Zhang, et al., “Four New Observational  $H(z)$  Data From Luminous Red Galaxies of Sloan Digital Sky Survey Data Release Seven”, *Res. Astron. Astrophys.* **14**, 1221, (2014), <https://doi.org/10.1088/1674-4527/14/10/002>
- [103] R. Jimenez, et al., “Constraints on the Equation of State of Dark Energy and Hubble Constant from Stellar Ages and the cosmic Microwave Background”, *Astrophys. Jour.* **593**, 622, (2003), <https://doi.org/10.1086/376595>
- [104] J. Simon, L. Verde and R. Jimenez, “Constraints on the redshift dependence of the dark energy potential”, *Phys. Rev. D* **71**, 123001, (2005), <https://doi.org/10.1103/PhysRevD.71.123001>

- 10.1103/PhysRevD.71.123001
- [105] D. Stern, et al., "Cosmic Chronometers: Constraining the Equation of State of Dark Energy. I:  $H(z)$  Measurements", *JCAP* **02**, 008, (2010), <https://doi.org/10.1088/1475-7516/2010/02/008>
- [106] Moresco et al., "Improved constraints on the expansion rate of the Universe up to  $z \sim 1.1$  from the spectroscopic evolution of the cosmic chronometers", *JCAP*, **08**, 006, (2012), <https://doi.org/10.1088/1475-7516/2012/08/006>
- [107] T. M. C. Abbott, et al. "Dark Energy Survey Year 1 Results: A Precise  $H_0$  Estimate from DES Y1, BAO, and D/H Data", *Month. Not. R. Astron. Soc.*, **480**, 3, 3879–88, (2018). <https://doi.org/10.1093/mnras/sty1939>
- [108] Metin Ata, et al. "The Clustering of the SDSS-IV Extended Baryon Oscillation Spectroscopic Survey DR14 Quasar Sample: First Measurement of Baryon Acoustic Oscillations between Redshift 0.8 and 2.2", *Month. Not. R. Astron. Soc.*, **473**, 4, 4773–94, (2018). <https://doi.org/10.1093/mnras/stx2630>.
- [109] E. Aubourg, et al. "Cosmological Implications of Baryon Acoustic Oscillation Measurements", *Phys. Rev. D*, **92**, 12, 123516, (2015) . <https://doi.org/10.1103/PhysRevD.92.123516>
- [110] J. E. Bautista, et al. 'Measurement of Baryon Acoustic Oscillation Correlations at  $z = 2.3$  with SDSS DR12 Ly  $\alpha$  -Forests'. *Astron. & Astrophys.*, **603**, A12, (2017). <https://doi.org/10.1051/0004-6361/201730533>.
- [111] M. Betoule, et al. 'Improved Cosmological Constraints from a Joint Analysis of the SDSS-II and SNLS Supernova Samples'. *Astron. & Astrophys.*, **568**, A22, 32, (2014) . <https://doi.org/10.1051/0004-6361/201423413>.
- [112] D.Brout et al. "The Pantheon+ Analysis: Cosmological Constraints." *Astrophys. Jour.*, **938**, 2, 110, (2022). <http://doi.org/10.3847/1538-4357/ac8e04>
- [113] D. Scolnic et al. 'The Pantheon+ Analysis: The Full Data Set and Light-Curve Release'. *Astrophys. Jour.*, **938**, 2, 113, (2022). <https://doi.org/10.3847/1538-4357/ac8b7a>.
- [114] S. Alam, et al. "Completed SDSS-IV Extended Baryon Oscillation Spectroscopic Survey: Cosmological Implications from Two Decades of Spectroscopic Surveys at the Apache Point Observatory". *Phys. Rev. D*, **103**, 8, 083533, (2021) . <https://doi.org/10.1103/PhysRevD.103.083533>.
- [115] D.J. Eisenstein, et al. 'Detection of the Baryon Acoustic Peak in the Large-Scale Correlation Function of SDSS Luminous Red Galaxies', *Astrophys. Jour.*, **633**, 2, 560–74, (2005). <https://doi.org/10.1086/466512>.
- [116] W.J. Percival, et al. 'Baryon Acoustic Oscillations in the Sloan Digital Sky Survey Data Release 7 Galaxy Sample'. *MNRAS*, **401**, 4, 2148–68,(2010). <https://doi.org/10.1111/j.1365-2966.2009.15812.x>.
- [117] C. Blake, and K. Glazebrook. 'Probing Dark Energy Using Baryonic Oscillations in the Galaxy Power Spectrum as a Cosmological Ruler', *Astrophys. Jour.*, **594**, 2, 665–73, (2003). <https://doi.org/10.1086/376983>.
- [118] W. Hu, and N. Sugiyama. 'Small-Scale Cosmological Perturbations: An Analytic Approach', *Astrophys. Jour.* , **471** , 2, 542–570, (1996). <http://dx.doi.org/10.1086/177989>.
- [119] D.J Eisenstein., and W. Hu. 'Baryonic Features in the Matter Transfer Function'. *Astrophys. Jour.*, **496**, 2, 605–14, (1998). <https://doi.org/10.1086/305424>
- [120] K. S. Dawson, et al. 'The SDSS-IV extended baryon oscillation spectroscopic survey: overview and early data', *Astron. Jour.*, **151**, 2, 44, (2016). <https://doi.org/10.3847/0004-6256/151/2/44>.
- [121] DESI Collaboration et al., "DESI DR2 Results II: Measurements of Baryon Acoustic Oscillation and Cosmological Constraints". arXiv:2503.14738v2 (2025) . <https://doi.org/10.48550/arXiv.2503.14738>.
- [122] A. G. Abac, et al. (The LIGO Scientific Collaboration, the Virgo Collaboration, the KAGRA Collaboration), "GWTC-4.0: Tests of General Relativity. I. Overview and General Tests", arXiv:2603.19019, (2026), <https://doi.org/10.48550/arXiv.2603.19019>
- [123] A. G. Abac, et al. (The LIGO Scientific Collaboration, the Virgo Collaboration, the KAGRA Collaboration), "GWTC-4.0: Tests of General Relativity. II. Parameterized Tests", arXiv:2603.19020, (2026), <https://doi.org/10.48550/arXiv.2603.19020>
- [124] S. Weinberg, "Cosmology", Oxford university press, (2008)
- [125] D. W. Hogg, et al. "Data Analysis Recipes: Fitting a Model to Data," arXiv:1008.4686, (2010), <https://doi.org/10.48550/ARXIV.1008.4686>
- [126] D. W. Hogg and D. Foreman-Mackey, "Data Analysis Recipes: Using Markov Chain Monte Carlo". *Astrophys. Jour.* **236**, 11, (2018) <https://doi.org/10.3847/1538-4365/aab76e>
- [127] Gravitational Wave Open Science Center (GWOSC):<https://gwosc.org/eventapi/html/allevvents/>
- [128] X. Zhang, "Gravitational wave standard sirens and cosmological parameter measurement", *Sci. China-Phys. Mech. Astron.* **62**, 110431, (2019), <https://doi.org/10.1007/s11433-019-9445-7>
- [129] R. Gen Cai and T. Yang, "Estimating cosmological parameters by the simulated data of gravitational waves from the Einstein Telescope", *Phys. Rev. D* **95**, 044024, (2017), <https://doi.org/10.1103/PhysRevD.95.044024>
- [130] M. D. Hoffman, and A. Gelman, 'The No-U-Turn Sampler: Adaptively setting path lengths in Hamiltonian Monte Carlo' *Journal of Machine Learning Research*, **15**, 1593–1623, (2014). <https://dl.acm.org/doi/10.5555/2627435.2638586> <https://arxiv.org/abs/1111.4246>
- [131] A. Lewis, and S. Bridle. 'Cosmological Parameters from CMB and Other Data: A Monte Carlo Approach'. *Phys. Rev. D*, **66**, 10, 103511, (2002). <https://doi.org/10.1103/PhysRevD.66.103511>.
- [132] C. A. Lin and M. Kilbinger, "A new model to predict weak-lensing peak counts II. Parameter constraint strategies", *A&A* **583**, A70, (2015), <https://doi.org/10.1051/0004-6361/201526659>
- [133] S. De, C. M. Biwer, C. D. Capano, A. H. Nitz and D. A. Brown, "Posterior samples of the parameters of binary black holes from Advanced LIGO, Virgo's second observing run", *Sci Data* **6**, 81 (2019), <https://doi.org/10.1038/s41597-019-0086-6>
- [134] D. Brout, et al., "The Pantheon+ Analysis: Cosmological Constraints", *Astrophys. Jour.*, **938**, 110, <https://doi.org/10.3847/1538-4357/ac8e04>
- [135] Planck Collaboration, et al. "Planck 2018 Results:VI. Cosmological Parameters (Corrigendum)", *Astron. and Astrophys.*, **652**, C4, (2021). <https://doi.org/10.1051/0004-6361/201833910e>.

- [136] Planck Collaboration, et al. “Planck 2018 Results:I. Overview and the cosmological legacy of Planck”, *Astron. and Astrophys.*, **641**, A1, (2020). <https://doi.org/10.1051/0004-6361/201833880>
- [137] Adam G. Riess, et al. “Cosmic Distances Calibrated to 1 percent Precision with Gaia EDR3 Parallaxes and Hubble Space Telescope Photometry of 75 Milky Way Cepheids Confirm Tension with  $\Lambda$ CDM”. *Astrophys. Jour. Lett.*, **908**, 1, L6, (2021). <https://doi.org/10.3847/2041-8213/abdbaf>.
- [138] “Everything in Natural Unit (High-Energy Physics)”, <https://github.com/ymzhong/naturalunit>

## Appendix A: Derivations of k-essence Theory

The k-essence action is

$$S_k[\phi, g^{\mu\nu}] = \int d^4x \sqrt{-g} \mathcal{L}(X, \phi) \quad (\text{A1})$$

where the canonical kinetic term  $X = \frac{1}{2} g^{\mu\nu} \nabla_\mu \phi \nabla_\nu \phi$ . As  $\phi$  is a scalar field, so we can write,  $X = \frac{1}{2} g^{\mu\nu} \partial_\mu \phi \partial_\nu \phi$ .

Now the variation of the above action  $S_k[\phi, g^{\mu\nu}]$  can be derived in two parts, one with respect to with respect to the metric  $g^{\mu\nu}$  and another with respect to  $\phi$  as :

$$\delta S_k[\phi, g^{\mu\nu}] = \delta S_k[\phi, g^{\mu\nu}]|_{g^{\mu\nu}} + \delta S_k[\phi, g^{\mu\nu}]|_\phi \quad (\text{A2})$$

Here  $\delta S_k[\phi, g^{\mu\nu}]|_{g^{\mu\nu}}$  and  $\delta S_k[\phi, g^{\mu\nu}]|_\phi$  are the variations of the k-essence action  $S_k[\phi, g^{\mu\nu}]$  with respect to the metric  $g^{\mu\nu}$  and the scalar field  $\phi$  respectively. Now the first term in A2 can be expressed as,

$$\delta S_k[\phi, g^{\mu\nu}]|_{g^{\mu\nu}} = \int d^4x \sqrt{-g} \delta g^{\mu\nu} \frac{1}{2} \left[ \mathcal{L}_X \nabla_\mu \phi \nabla_\nu \phi - g^{\mu\nu} \mathcal{L} \right] \quad (\text{A3})$$

Therefore, the energy-momentum tensor  $T_{\mu\nu}$  is:

$$T_{\mu\nu} = - \frac{2}{\sqrt{-g}} \frac{\delta S_k[\phi, g^{\mu\nu}]|_{g^{\mu\nu}}}{\delta g^{\mu\nu}}$$

or,  $T_{\mu\nu} = g_{\mu\nu} \mathcal{L} - \mathcal{L}_X \nabla_\mu \phi \nabla_\nu \phi \quad (\text{A4})$

As  $\phi$  is a scalar field then we also can write [51]

$$T_{\mu\nu} = g_{\mu\nu} \mathcal{L} - \mathcal{L}_X \partial_\mu \phi \partial_\nu \phi \quad (\text{A5})$$

On the other hand, the second term of A2 can be expressed as:

$$\begin{aligned} \delta S_k[\phi, g^{\mu\nu}]|_\phi &= - \int d^4x \sqrt{-g} \left[ (\mathcal{L}_{XX} \nabla^\mu \phi \nabla_\nu \phi \right. \\ &\quad \left. + \mathcal{L}_X g^{\mu\nu}) \nabla_\mu \nabla_\nu \phi + 2X \mathcal{L}_{X\phi} - \mathcal{L}_\phi \right] \delta \phi \end{aligned} \quad (\text{A6})$$

where  $\mathcal{L}_X \equiv \frac{\partial \mathcal{L}}{\partial X}$ ,  $\mathcal{L}_{X\phi} \equiv \frac{\partial^2 \mathcal{L}}{\partial X \partial \phi}$ ,  $\mathcal{L}_{XX} \equiv \frac{\partial^2 \mathcal{L}}{\partial X^2}$  and  $\mathcal{L}_\phi \equiv \frac{\partial \mathcal{L}}{\partial \phi}$ .

Therefore, the scalar field equation of motion is [51]:

$$- \frac{1}{\sqrt{-g}} \frac{\delta S_k}{\delta \phi} = \bar{G}^{\mu\nu} \nabla_\mu \phi \nabla_\nu \phi + 2X \mathcal{L}_{X\phi} - \mathcal{L}_\phi \quad (\text{A7})$$

where  $\bar{G}^{\mu\nu}$  is the effective emergent metric which can be defined as:

$$\bar{G}^{\mu\nu} = g^{\mu\nu} \mathcal{L}_X + \mathcal{L}_{XX} \nabla^\mu \phi \nabla^\nu \phi \quad (\text{A8})$$

with  $1 + \frac{2X \mathcal{L}_{XX}}{\mathcal{L}_X} > 0$  and the velocity of sound  $c_s^2 = \left( 1 + 2X \frac{\mathcal{L}_{XX}}{\mathcal{L}_X} \right)^{-1}$  [51]. Here “Bar” ( $\bar{\phantom{x}}$ ) sign does not indicate the background geometry.

Now the inverse of the effective emergent metric is expressed as:

$$\bar{G}_{\mu\nu} = \frac{\mathcal{L}_X}{c_s} \left[ g_{\mu\nu} - c_s^2 \frac{\mathcal{L}_{XX}}{\mathcal{L}_X} \nabla_\mu \phi \nabla_\nu \phi \right] \quad (\text{A9})$$

Using the relation  $\tilde{G}_{\mu\nu} = \frac{c_s}{\mathcal{L}_X} \bar{G}_{\mu\nu}$ , we get

$$\tilde{G}_{\mu\nu} = g_{\mu\nu} - \frac{\mathcal{L}_{XX}}{\mathcal{L}_X + 2X \mathcal{L}_{XX}} \nabla_\mu \phi \nabla_\nu \phi \quad (\text{A10})$$

Here “Tilde” ( $\tilde{\phantom{x}}$ ) sign is not indicating the trace reversed terms.

## Appendix B: Non-Zero Curvature tensors From Background Universe

In section III B we have already considered the conformal flat FLRW universe with scalar-tensor perturbation in Eq.(28). The background spacetime metric is (already mentioned in Eq.(30))

$$ds^2 = \bar{g}_{\mu\nu} dx^\mu dx^\nu = a^2(\eta) [d\eta^2 - \delta_{ij} dx^i dx^j] \quad (\text{B1})$$

Here  $a^2(\eta)$  is the scale factor, and the conformal time  $\eta$  is defined in form of cosmic time coordinate  $t$  as follows, [29, 54]

$$\eta \equiv \int \frac{dt}{a(t)} \quad (\text{B2})$$

The non-zero background connection coefficients are

$$\begin{aligned} \bar{\Gamma}_{00}^0 &= (a'/a) = \mathcal{H} \\ \bar{\Gamma}_{ij}^0 &= \mathcal{H} \delta_{ij} \\ \bar{\Gamma}_{0j}^i &= \mathcal{H} \delta_j^i \end{aligned} \quad (\text{B3})$$

So the non-zero components of background Riemann tensors can be calculated as:

$$\begin{aligned} \bar{R}_{0i0j} &= (aa'' - a'^2) \delta_{ij} = a^2 \mathcal{H}' \delta_{ij} \\ \bar{R}_{i00j} &= -a^2 \mathcal{H}' \delta_{ij} \\ \bar{R}_{ijkl} &= -a'^2 (\delta_{ik} \delta_{jl} - \delta_{il} \delta_{jk}) \\ &= -a^2 \mathcal{H}^2 (\delta_{ik} \delta_{jl} - \delta_{il} \delta_{jk}) \end{aligned} \quad (\text{B4})$$

The non-zero components of the background Ricci tensors are

$$\begin{aligned} \bar{R}_{00} &= -3 \left( \frac{a''}{a} - \frac{a'^2}{a^2} \right) = -3\mathcal{H}' \\ \bar{R}_{ij} &= \left( \frac{a''}{a} + \frac{a'^2}{a^2} \right) \delta_{ij} = (\mathcal{H}' + 2\mathcal{H}^2) \delta_{ij} \end{aligned} \quad (\text{B5})$$

and the background Ricci scalar is

$$\bar{R} = - \frac{6}{a^2} \left( \frac{a''}{a} \right) = - \frac{6}{a^2} (\mathcal{H}' + \mathcal{H}^2) \quad (\text{B6})$$

Here  $\mathcal{H}$  is the conformal or comoving Hubble parameter, i.e.  $\mathcal{H} \equiv \mathcal{H}(\eta)$ . It can be defined in form of  $a(\eta)$  as follows:

$$\mathcal{H} \equiv \left( \frac{a'}{a} \right) \quad (\text{B7})$$

and note that,

$$\mathcal{H}' \equiv \left(\frac{a'}{a}\right)' = \frac{a''}{a} - \left(\frac{a'}{a}\right)^2 = \frac{a''}{a} - \mathcal{H}^2 \quad (\text{B8})$$

where ‘‘prime’’ ( $\equiv \partial_\eta$ ) denotes the first order derivative with respect to the conformal time.

Now here we consider an additional matter action  $S_m$  with the following definition,  $S_m = \int d^4x \sqrt{-g} \mathcal{L}_m$ , where  $\mathcal{L}_m$  is a matter Lagrangian. Therefore the total action will be,

$$S_{total} = S + S_m \quad (\text{B9})$$

where  $S$  is the action that is already mention in Eq.(16).

Now according to Ref.[48], we have the following total background energy-momentum tensor for perfect fluid consideration,

$$\bar{T}_{\mu\nu} = (\bar{\rho} + \bar{P})\bar{u}_\mu\bar{u}_\nu - \bar{P}\bar{g}_{\mu\nu} \quad (\text{B10})$$

where the background four-velocity vector  $\bar{u}_\mu = \frac{\partial_\mu \phi_0}{\sqrt{2\bar{X}}}$ , which satisfy the normalization condition,  $\bar{u}_\mu\bar{u}^\mu = 1$ ,  $\bar{\rho} = (\bar{\rho}_\phi + \bar{\rho}_m)$  and  $\bar{P} = (\bar{P}_\phi + \bar{P}_m)$  is the background energy density and pressure respectively. Here  $\bar{\rho}_\phi$  and  $\bar{P}_\phi$  is the k-essence background scalar field energy density and pressure (already defined in Eq.(46)) respectively.

So using the conformal flat FLRW background metric in Eq.(B1), and the pressureless dark matter, according to the cold dark matter (CDM) model, i.e.  $\bar{P}_m = 0$ , we express the following form of the conformal Friedmann equations,

$$\mathcal{H}^2 = \frac{8\pi G}{3} a^2 \bar{\rho} = \frac{8\pi G}{3} a^2 (\bar{\rho}_\phi + \bar{\rho}_m)$$

$$\text{and } \mathcal{H}' = -\frac{4\pi G}{3} a^2 (\bar{\rho} + 3\bar{P}) = -\frac{4\pi G}{3} a^2 (\bar{\rho}_\phi + \bar{\rho}_m + 3\bar{P}_\phi) \quad (\text{B11})$$

### Appendix C: Observational Data Sets

The Hubble parameter values  $H(z)$  listed in Table (II), are collected from various observational studies covering a redshift range approximately from  $z \sim 0.07$  to  $z \sim 1.965$ . These measurements are obtained using the cosmic chronometer (or differential age) technique, which determines  $H(z)$  by evaluating the age difference between passively evolving galaxies at distinct redshifts.

$z$	$H(z)$	$\sigma_{H,i}$	Refs.
0.07	69.0	$\pm 19.60$	[102]
0.0708	69.0	$\pm 19.68$	[17]
0.09	69.0	$\pm 12.0$	[103]
0.12	68.6	$\pm 26.2$	[102]
0.17	83.0	$\pm 8.00$	[104]
0.179	75.0	$\pm 4.0$	[106]
0.199	75.0	$\pm 5.0$	[106]
0.20	72.9	$\pm 29.6$	[17]
0.27	77.0	$\pm 14.0$	[104]
0.28	88.8	$\pm 36.6$	[17]
0.352	83.0	$\pm 14.0$	[106]
0.38	81.2	$\pm 2.2$	[108]
0.3802	83.0	$\pm 14.0$	[109]
0.4	95.0	$\pm 17.0$	[104]
0.4004	77.0	$\pm 10.2$	[109]
0.4247	87.1	$\pm 11.2$	[109]
0.4497	92.8	$\pm 12.9$	[109]
0.47	89.0	$\pm 50.0$	[110]
0.4783	80.9	$\pm 9.0$	[109]
0.48	97.0	$\pm 62.0$	[105]
0.51	90.9	$\pm 2.1$	[108]
0.593	104.0	$\pm 13.0$	[106]
0.61	98.96	$\pm 2.20$	[108]
0.68	92.00	$\pm 8.0$	[106]
0.781	105.0	$\pm 12.0$	[106]
0.875	125.0	$\pm 17.0$	[106]
0.88	99.0	$\pm 40.0$	[105]
0.9	117.0	$\pm 23.0$	[104]
1.037	154.0	$\pm 20.0$	[106]
1.3	168.0	$\pm 17.0$	[104]
1.363	160.0	$\pm 33.6$	[111]
1.43	177.0	$\pm 18.0$	[104]
1.53	140.0	$\pm 14.0$	[104]
1.75	202.0	$\pm 40.0$	[104]
1.965	186.5	$\pm 50.4$	[111]

Table II: Here the  $H(z)$  value is derived from the cosmic chronological method or the differential age approach, with the relevant references cited accordingly. The unit of  $H(z)$  is  $km.s^{-1}.Mpc^{-1}$ , ‘CC’ indicates that .

We analyze two separate BAO datasets in this study. The first dataset, referred to as SDSSBAO, consists of 8 data points obtained from the SDSS. The second dataset, called DESIBAO, includes 9 data points from the DESI. For the DESI dataset, we specifically use the most recent DR2 provided by the collaboration. The combination of these two datasets, SDSSBAO and DESIBAO, is collectively referred to as the BAO dataset in our analysis. The detailed values for both datasets are presented in Table (III) and Table (IV).

$\tilde{z}$	<b>0.15</b>	<b>0.38</b>	<b>0.51</b>	<b>0.70</b>	<b>0.85</b>	<b>1.48</b>	<b>2.33</b>	<b>2.33</b>
$D_V(\tilde{z})/r_d$	$4.47 \pm 0.17$	-	-	-	$18.33^{+0.57}_{-0.62}$	-	-	-
$D_M(\tilde{z})/r_d$	-	$10.23 \pm 0.17$	$13.36 \pm 0.21$	$17.86 \pm 0.33$	-	$30.69 \pm 0.80$	$37.6 \pm 1.9$	$37.3 \pm 1.7$
$D_H(\tilde{z})/r_d$	-	$25.00 \pm 0.76$	$22.33 \pm 0.58$	$19.33 \pm 0.53$	-	$13.26 \pm 0.55$	$8.93 \pm 0.28$	$9.08 \pm 0.34$

Table III: SDSSBAO Dataset

$\tilde{z}$	$D_V(\tilde{z})/r_d$	$D_M(\tilde{z})/r_d$	$D_H(\tilde{z})/r_d$
0.295	$7.942 \pm 0.075$	-	-
0.510	$12.720 \pm 0.099$	$13.588 \pm 0.167$	$21.863 \pm 0.425$
0.706	$16.050 \pm 0.110$	$17.351 \pm 0.177$	$19.455 \pm 0.330$
0.922	$19.656 \pm 0.105$	$21.648 \pm 0.178$	$17.577 \pm 0.213$
0.934	$19.721 \pm 0.091$	$21.576 \pm 0.152$	$17.641 \pm 0.193$
0.955	$20.008 \pm 0.183$	$21.707 \pm 0.335$	$17.803 \pm 0.297$
1.321	$24.252 \pm 0.174$	$27.601 \pm 0.318$	$14.176 \pm 0.221$
1.484	$26.055 \pm 0.398$	$30.512 \pm 0.760$	$12.817 \pm 0.516$
2.330	$31.267 \pm 0.256$	$38.988 \pm 0.531$	$8.632 \pm 0.101$

Table IV: DESI BAO Dataset (DR2)

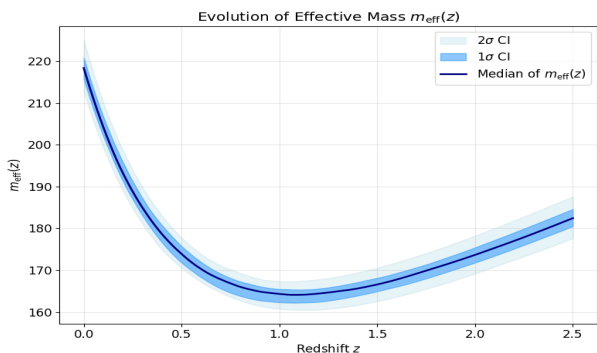
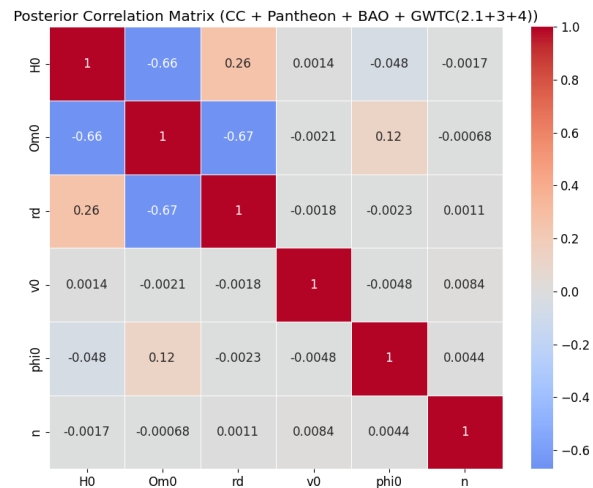
Figure 7: Evolution of the effective mass term  $m_{eff}$  as a function of redshift  $z$  for the observational datasets CC + BAO + GWTC(2.1 + 3 + 4)

Figure 9: Bayesian inference correlation heatmap structure for the observational datasets CC + Pantheon + BAO + GWTC(2.1 + 3 + 4)



Figure 8: Bayesian inference correlation heatmap structure for the observational datasets CC + BAO + GWTC(2.1 + 3 + 4)